Stem Cell Reports
Article
OPEN ACCESS

Acellular Lung Scaffolds Direct Differentiation of Endoderm to Functional Airway Epithelial Cells: Requirement of Matrix-Bound HS Proteoglycans

Sharareh Shojaie,[1,2] Leonardo Ermini,[1] Cameron Ackerley,[1] Jinxia Wang,[1] Stephanie Chin,[3] Behzad Yeganeh,[1] Mélanie Bilodeau,[4] Manpreet Sambi,[5] Ian Rogers,[2,5] Janet Rossant,[4,6] Christine E. Bear,[2,3] and Martin Post[1,2,*]
[1]Program in Physiology and Experimental Medicine, Peter Gilgan Centre for Research and Learning, Hospital for Sick Children, Toronto, ON M5G 0A4, Canada
[2]Department of Physiology, Faculty of Medicine, University of Toronto, Toronto, ON M5S1A8, Canada
[3]Program in Molecular Structure and Function, Peter Gilgan Centre for Research and Learning, Hospital for Sick Children, Toronto, ON M5G 0A4, Canada
[4]Program in Developmental and Stem Cell Biology, Peter Gilgan Centre for Research and Learning, Hospital for Sick Children, Toronto, ON M5G 0A4, Canada
[5]Lunenfeld-Tanenbaum Research Institute, Mount Sinai Hospital, Toronto, ON M5G 1X5, Canada
[6]Department of Molecular Genetics, University of Toronto, Toronto, ON M5S 1A8, Canada
*Correspondence: martin.post@sickkids.ca
http://dx.doi.org/10.1016/j.stemcr.2015.01.004

SUMMARY

Efficient differentiation of pluripotent cells to proximal and distal lung epithelial cell populations remains a challenging task. The 3D extracellular matrix (ECM) scaffold is a key component that regulates the interaction of secreted factors with cells during development by often binding to and limiting their diffusion within local gradients. Here we examined the role of the lung ECM in differentiation of pluripotent cells in vitro and demonstrate the robust inductive capacity of the native lung matrix alone. Extended culture of stem cell-derived definitive endoderm on decellularized lung scaffolds in defined, serum-free medium resulted in differentiation into mature airway epithelia, complete with ciliated cells, club cells, and basal cells with morphological and functional similarities to native airways. Heparitinase I, but not chondroitinase ABC, treatment of scaffolds revealed that the differentiation achieved is dependent on heparan sulfate proteoglycans and its bound factors remaining on decellularized scaffolds.

INTRODUCTION

Lineage restriction of pluripotent stem cells (PSCs) is a dynamic process mediated by many environmental components that include growth factors, cell-matrix interactions, cell-cell signaling, and mechanical forces (Daley et al., 2008; Discher et al., 2009). Understanding how these components combine and control cell fate in vivo will allow recapitulation of niche microenvironments in vitro and support lineage-specific differentiation and generation of target cell populations. Recent reports have attempted to capture the lung developmental milieu with the addition of soluble growth factors in monolayer cultures. Success in achieving differentiation to lung epithelial cells has employed a stepwise lineage restriction strategy to first achieve definitive endoderm, followed by anterior foregut endoderm, and finally lung progenitor cells with positive expression for the homeodomain-containing transcription factor NKX2-1. NKX2-1$^+$ lung progenitors were further differentiated to airway or alveolar epithelia with some success using continued supplementation of monolayer cultures with inductive factors (Ghaedi et al., 2013; Green et al., 2011; Huang et al., 2014; Jensen et al., 2012; Longmire et al., 2012; Mou et al., 2012; Wong et al., 2012). Repopulation of decellularized scaffolds has been used as an end-point assay to assess regenerative potential of predifferentiated cells (Ghaedi et al., 2013; Huang et al., 2014; Jensen et al., 2012; Longmire et al., 2012). Gilpin et al. (2014) recently reported the importance of the matrix environment for maintaining lung progenitor identity, but again using predifferentiated NKX2-1$^+$ lung progenitor cells and growth factor-supplemented culture media, precluding assessment of the scaffolds alone on differentiation. To our knowledge, no reports have assessed the inductive capacity of the lung extracellular matrix (ECM) alone during early lung specification.

Here we present a strategy to examine the role of the lung ECM in differentiation of pluripotent cells in vitro and show the inductive capacity of decellularized lung scaffolds alone in directing differentiation to functional airway epithelial cells. Decellularized lung scaffolds were seeded with embryonic stem cell-derived endoderm under defined, serum-free conditions to investigate the sole potential of the lung ECM in promoting lineage-specific differentiation. We demonstrate the importance of a 3D matrix environment with site-specific cues that are bound to heparan-sulfate proteoglycans for achieving robust differentiation to mature and functional airway epithelial cells.

RESULTS

Endodermal Cells Differentiate to NKX2-1$^+$/SOX2$^+$ Early Proximal Lung Progenitors with Culture on Decellularized Scaffolds

To investigate cell-ECM interactions during lung specification, we isolated decellularized lung scaffolds from adult

rats. Rapid and complete decellularization was achieved using a 3-[(3-cholamidopropyl)dimethylammonio]-1-propanesulfonate (CHAPS)-based decellularization solution (Figure S1 available online). Tissue staining, electron microscopy (EM), tensile testing, and DNA and immunoblot analyses of decellularized scaffolds confirmed removal of all host cells and preservation of matrix proteins (Figures S1A–S1J).

During embryonic development, lung-specific endoderm progenitors originate from definitive anterior endoderm found in the developing foregut (Murry and Keller, 2008; Zorn and Wells, 2009). Therefore, we first generated definitive endoderm from mouse embryonic stem cells (ESCs) using activin A (Gouon-Evans et al., 2006; Kubo et al., 2004) and isolated an enriched population of endodermal cells by fluorescence-activated cell sorting for coexpression of CXCR4 and cKIT (Figures S2A and S2B). Sorted cells were seeded onto 350 μm thick sections of decellularized scaffolds and cultured in a supportive base media for up to 3 weeks without the addition of exogenous factors. To better recapitulate the lung microenvironment, we maintained cell-matrix constructs under air-liquid interface (ALI) culture conditions (Figure S2C). By 7 days of culture, seeded endodermal cells presented a pattern of organization reminiscent of the developing lung, lined by basement membrane proteins collagen IV and laminin (Figures S2D and S2E). Tubule structures were formed, and over half of the seeded population coexpressed pan-epithelial cell markers CDH1 and panKRT (Figure S2F). RT-PCR analysis showed maintenance of endoderm transcription factor *Foxa2* expression for the duration of culture on scaffolds (Figure 1B). *Nkx2-1* is an important transcriptional regulator of the lung that is one of the earliest markers for emergence of lung-specific endodermal cells (Kimura et al., 1996; Minoo et al., 1999). There was upregulation of *Nkx2-1* after 7 days of culture on scaffolds, and expression was maintained for up to 21 days (Figure 1C); proximal (*Sox2*) and distal (*Sox9*) epithelial progenitor markers were both detected at the mRNA level, although *Sox2* levels were greater (Figures 1D and 1E).

Using an *Nkx2-1*^{mCherry} ESC line with a nondisruptive mCherry reporter gene knockin (Bilodeau et al., 2014), we were able to capture the lung epithelial progenitor population as it emerged with culture on the scaffolds. Flow cytometric quantification revealed that 9.8% of cells expressed mCherry at day 7, and this percentage increased to 46.4% with extended culture on scaffolds at day 21 (Figures 1F and 1G). Elastase treatment was used to retrieve cells from scaffolds for flow cytometric analysis. Approximately 9.43×10^5 cells (n = 3) were recovered from each day 21-scaffold culture using this method, and each seeded scaffold culture generated approximately 4.38×10^5 NKX2-1$^+$ cells (n = 3) at day 21 (see Supplemental Experimental Procedures).

NXK2-1 is not specific to lung development as it is also a transcriptional regulator during thyroid and forebrain formation (Kimura and Deutsch, 2007). However, relative to expression of adult tissue, thyroid lineage markers *Tg* and *Pax8* and neuroectoderm marker *Olig2* were hardly detected in seeded scaffold cultures (Figure S2G). Expression of posterior endoderm lineage markers such as *Alb* (liver), *Pdx1* (pancreas), and *Foxa3* (posterior endoderm) was also not noted (Figure S2G). Immunofluorescent (IF) confocal analysis showed the presence of NKX2-1$^+$/SOX2$^+$/TRP63$^+$ airway basal stem cells in day 7 cultures (Figure 1H). A smaller population of distal lineage NKX2-1$^+$/SOX9$^+$ progenitor cells was also detected (Figure 1I). By day 21, majority of the emerging NKX2-1$^+$ cells coexpressed SOX2, while staining of SOX9 was not detected, indicating lineage restriction to the proximal airway (Perl et al., 2005; Que et al., 2009) (Figures 1J and 1K).

We conclude that decellularized lung scaffolds are able to support the adherence and organization of seeded endodermal cells and promote the upregulation of lung progenitor marker NKX2-1, with preference for the proximal airway lineage.

Prolonged Culture of Endodermal Cells on Lung Scaffolds Promotes Differentiation to Ciliated, Club, and Basal Epithelial Cells

To determine whether NKX2-1$^+$/SOX2$^+$ cells cultured on lung scaffolds alone were differentiating further to mature epithelia, seeded cells were examined for expression of proximal and distal lung epithelial cell markers (Figure 2A). RT-PCR analysis showed upregulated gene expression of proximal airway epithelia *Foxj1* (ciliated cell), *Scgb1a1* (club cell), *Trp63* (basal cell), and *Cftr* (Figure 2B), while expression of distal lung epithelial cell markers *Aqp5* (type I alveolar cell marker), *Sftpb*, and *Sftpc* (type II alveolar cell markers) were much lower (Figure 2C).

IF confocal microscopy of day 21 cell-matrix cultures revealed ciliated cells (FOXJ1$^+$, TUBB4A$^+$), club cells (CLDN10$^+$, SCGB1A1$^+$), and basal cells (TRP63$^+$, KRT5$^+$) (Figures 2D and S3A). Quantification of cells with positive immunostaining for lung lineage markers revealed 24.3% TUBB4A$^+$, 21.1% SCGB1A1$^+$, and 21.7% TRP63$^+$ cells at 21 days of culture on scaffolds (Figure 2E). EM analysis was used for high-magnification morphological analysis of differentiated epithelia. Seeded cells resembled that of native mouse airways (Figures 2F and 2G), where mature multiciliated cells were present among nonciliated secretory cells with rounded apical surfaces. Scanning and transmission EM analysis revealed tight junction-coupled pseudostratified columnar epithelial sheets (Figures 2F, 2H, and 2I).

A reduction in the number of TRP63$^+$ airway basal cells was observed by RT-PCR and by immunostaining at day 21 compared with day 7 (Figures 2B and 2E). This is

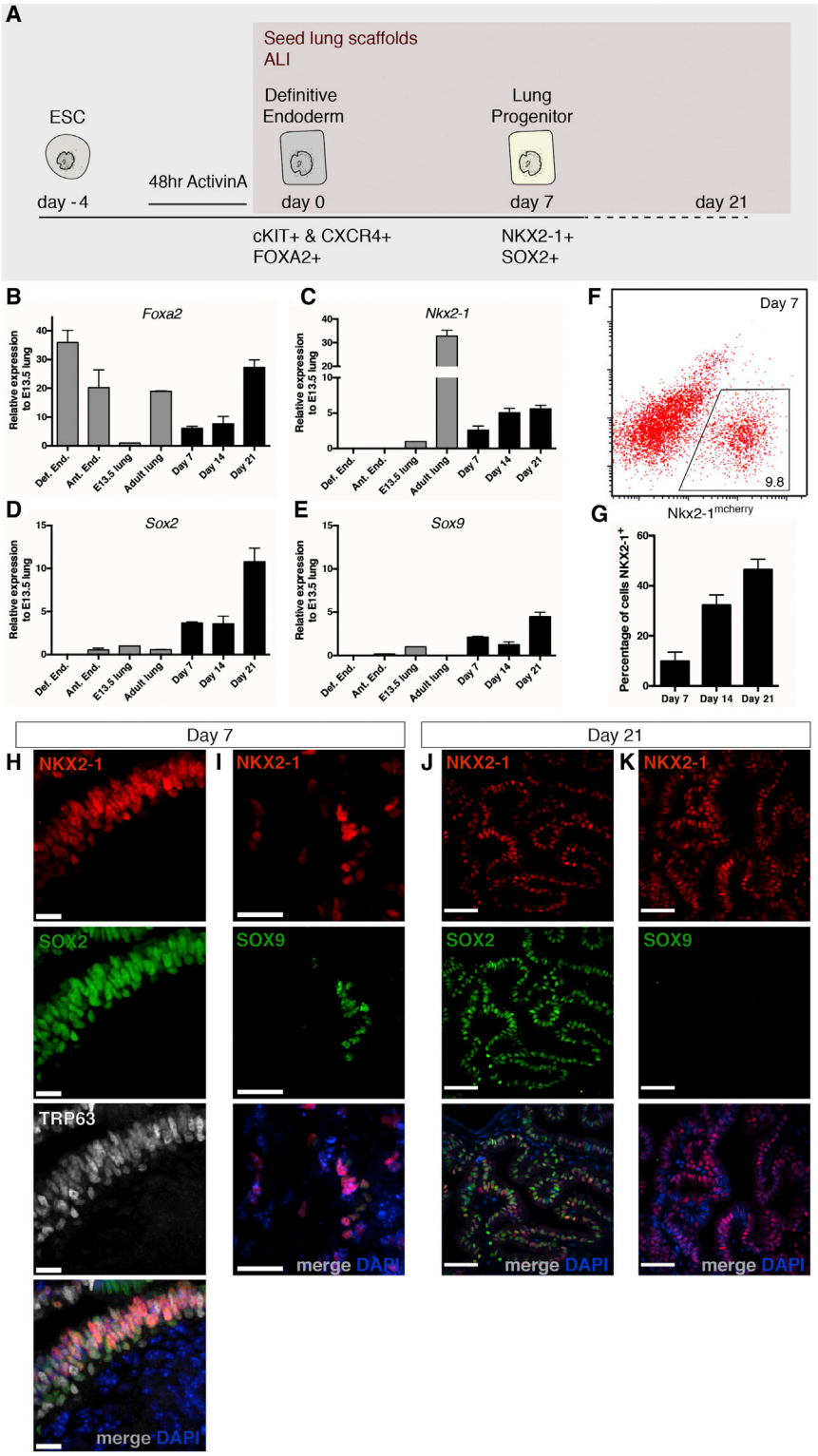

Figure 1. Seeded Endodermal Cells Differentiate to NKX2-1$^+$/SOX2$^+$ Proximal Lung Progenitors with Culture on Decellularized Scaffolds

(A) Schematic representation of differentiation to lung progenitor cells.

(B and C) Real-time PCR analysis reveals an upregulation of *Foxa2* and lung progenitor marker *Nkx2-1* expression. Expression is presented relative to E13.5 mouse lungs, mean ± SEM, n = 4 experiments.

(D and E) Proximal airway progenitor marker *Sox2* and distal alveolar progenitor marker *Sox9* were both detected, n = 4 experiments; with extended culture (day 21), *Sox2* expression is upregulated.

(F and G) NKX2-1$^{mcherry+}$ cells are quantified with flow cytometry. The proportion of NKX2-1$^+$ cells increases with extended culture at day 21 to 46.42% ± 3.6%, n = 3 experiments.

(H and I) Immunostaining of day 7 cultures shows the presence of NKX2-1$^+$/SOX2$^+$/TRP63$^+$ coexpressing airway basal stem cells. A small population of distal lineage NKX2-1$^+$/SOX9$^+$ progenitor cells is also present at this time point. (H) Scale bar represents 13 μm; (I) scale bar represents 25 μm.

(J and K) Immunostaining of day 21 cultures for NKX2-1, SOX2, and SOX9 reveals that the majority of NKX2-1$^+$ cells coexpress SOX2, while SOX9 protein expression is rare. Scale bar represents 50 μm.

See also Figures S1 and S2.

consistent with previously published work on the progenitor activity of airway basal cells (Hong et al., 2004; Rock et al., 2009; Zuo et al., 2014), suggesting that multipotent NKX2-1$^+$/SOX2$^+$/TRP63$^+$ basal stem cells in early cultures may be differentiating to club cells and ciliated cells lining the developing airway structures.

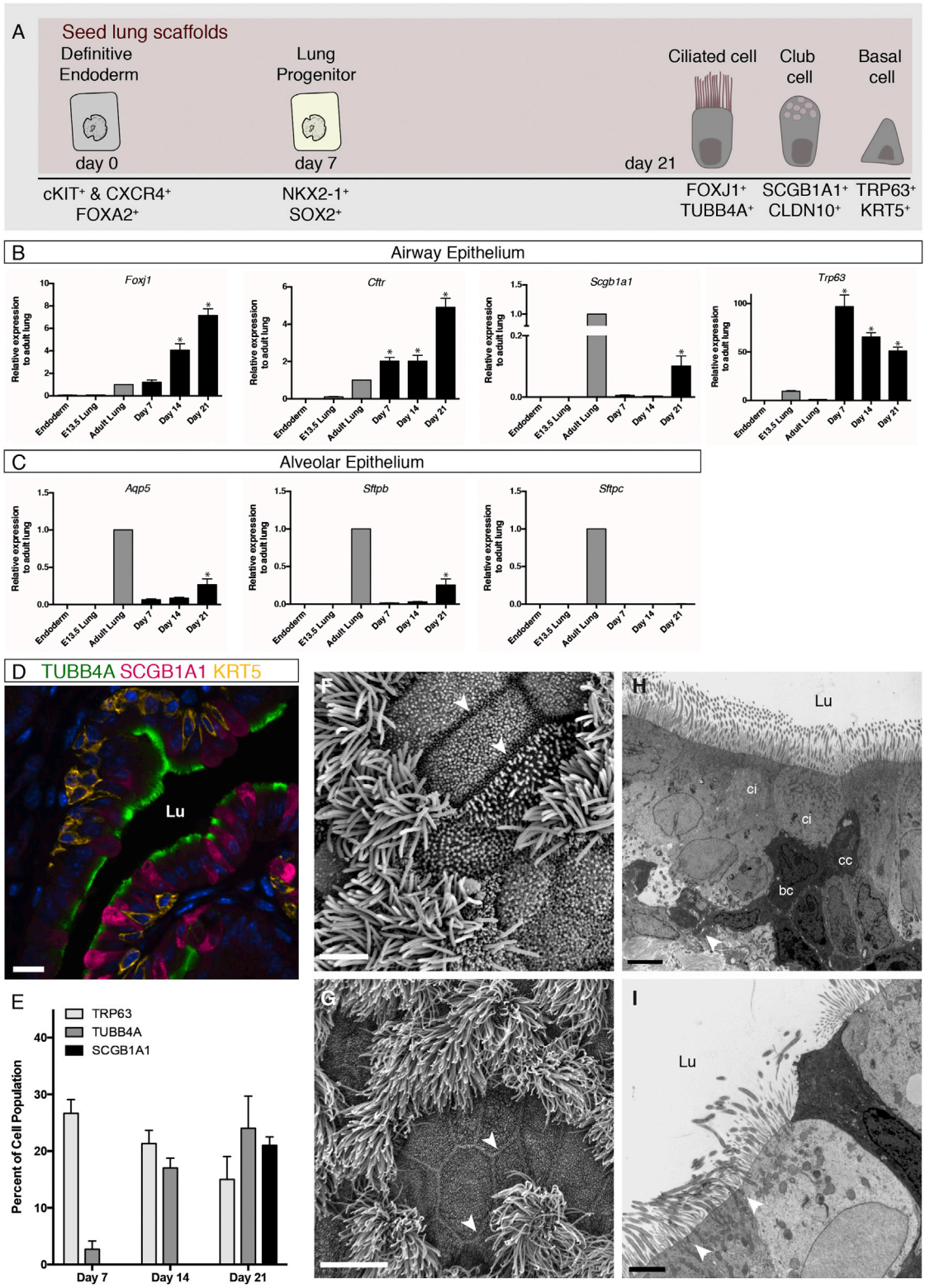

Figure 2. Extended Culture of Endodermal Cells on Lung Scaffolds Promotes Differentiation to Ciliated, Club, and Basal Airway Epithelial Cells

(A) Schematic representation of ESC differentiation to airway epithelial populations.

(legend continued on next page)

Decellularized scaffolds derived from mouse lungs seeded with definitive endodermal cells produced similar results to that obtained with rat lung scaffolds. Comparable cellular organization and differentiation was achieved using scaffolds generated from both the proximal and distal lung regions (Figures 3A and 3B). Tissue staining of day 21 culture sections obtained from various tissue depths demonstrated that decellularized scaffolds are completely repopulated after seeding (Figure S3B). Differentiation of definitive endoderm to airway epithelia using rat lung scaffolds was reproducible with two additional mouse ESC lines: G4 and 129/Ola (data not shown), as well as a rat ESC line (DAc8) (Figure S3C). Overall, decellularized adult lung scaffolds promote efficient differentiation of stem cell-derived definitive endoderm to airway epithelial cells.

Day 21 scaffold cultures were negative for pluripotency marker POU5F1, while maintaining definitive endoderm transcription factor FOXA2 expression (Figure 3C). In contrast to seeded scaffolds, endodermal cells cultured alone at ALI did neither form epithelial structures nor express any lung epithelial cell markers (Figure 3C). There was an increase in the number of apoptotic cells at day 21 compared with day 7, as apparent with transferase (TdT)-mediated dUTP nick end labeling (TUNEL) staining (Figure 3D) and flow cytometric analysis of recovered cells from scaffolds (data not shown). Apoptosis of cells that are not committed to a lung lineage with continued culture on scaffolds can partially explain the increase in the proportion of NKX2-1$^+$ cells at day 21 (Figure 1G). An increase in the number of differentiated cells with extended culture occurred in parallel with a decline in cell proliferation, as apparent with a reduction in Ki67$^+$ cells (Figure 3E).

To determine whether individual matrix proteins can promote lung-lineage differentiation with ALI culture, we seeded endodermal cells on individual matrix proteins: collagen I, collagen IV, fibronectin, laminin, and matrix substitute Matrigel (Figure 3F). RT-PCR analysis showed the upregulation of all endodermal lineage markers *Pax8*, *Foxa3*, *Pdx1*, and neuroectoderm marker *Olig2* on single matrix proteins compared with decellularized lung scaffolds (Figure 3G). Tissue staining and high-magnification transmission EM showed that no individual matrix protein or Matrigel was able to promote organization and lung lineage differentiation comparable to that achieved with lung scaffolds (Figures S4B and S4C). To determine whether the ability of scaffolds to promote lung lineage specification is organ specific, we seeded decellularized kidney scaffolds (mesoderm germ layer origin) with definitive endoderm and cultured them at ALI. However, definitive endoderm seeded at varied densities did not adhere and proliferate on kidney sections. This suggests that kidney-derived ECM is distinct from lung-derived ECM in its ability to support and promote endoderm-lineage specification (Figure S4D).

Differentiated Airway Epithelial Cultures on Lung Scaffolds Consist of Mature Ciliated and Club Cells with Cystic Fibrosis Transmembrane Conductance Regulator Function

Fundamental to airway mucociliary function, day 21 differentiated ciliated epithelial cells contained the appropriate 9+2 dynein arms of respiratory cilia (Figures 4A and 4B) and showed coordinated beating in culture (Movie S1). High-magnification analysis of day 21 differentiated club cells with transmission EM showed characteristic secretory droplets (El-Gawad and Westfall, 2000; Peão et al., 1993) (Figure 4C), and SCGB1A1 (club/Clara cell secretory protein) was detected by western blot analysis in the culture media (Figure 4D), suggesting that mature club cells are synthesizing and secreting SCGB1A1 into the airway lumen. Close examination of mature cultures also revealed the presence of pit structures reminiscent of emerging submucosal glands that function to adjust the flow of fluid and mucus secretions in the proximal segments of the respiratory tracts (Engelhardt et al., 1995; Smolich et al., 1978). Scaffold cultures showed an upregulation of mucin-producing cell marker *Muc5ac* with prolonged culture (Figure S3D). Numerous gland-like orifices were discovered with scanning EM analysis, and a strong PAS-positive stain was apparent in the developed submucosal tubules (Figures S3E and S3F).

(B and C) RT-PCR analysis reveals the expression of airway epithelial genes *Foxj1*, *Scgb1a1*, *TRP63*, and *Cftr*. Alveolar epithelial markers *Aqp5*, *Sftpb*, and *Sftpc* were detected at much lower levels, although *Aqp5* and *Sftpb* increased with extended culture. Gene expression is presented relative to adult lungs, mean ± SEM, n = 4 experiments, *p < 0.001.
(D) IF staining and confocal microscopic analysis of day 21 cell-matrix cultures showed mature airway epithelial populations: ciliated cells (TUBB4A$^+$), club cells (SCGB1A1$^+$), and basal cells (KRT5$^+$). Scale bar represents 50 μm.
(E) Cell proportions were quantified as percent of total cell population at days 7, 14, and 21, mean ± SEM, n = 3 experiments.
(F and G) Scanning EM image of the surface epithelia of day 21 cultures (F, scale bar represents 2.5 μm) displays mature tight junction-coupled (white arrowhead) ciliated and nonciliated cells with similar morphology to native mouse airways (G, scale bar represents 5 μm).
(H and I) Transmission EM analysis of day 21 tissue sections confirms the presence of tight junction-coupled (white arrowhead) ciliated cells (ci), club cells (cc), and basal cells (bc). (H) Scale bar represents 4 μm. (I) Scale bar represents 2 μm.
See also Figures S2 and S3.

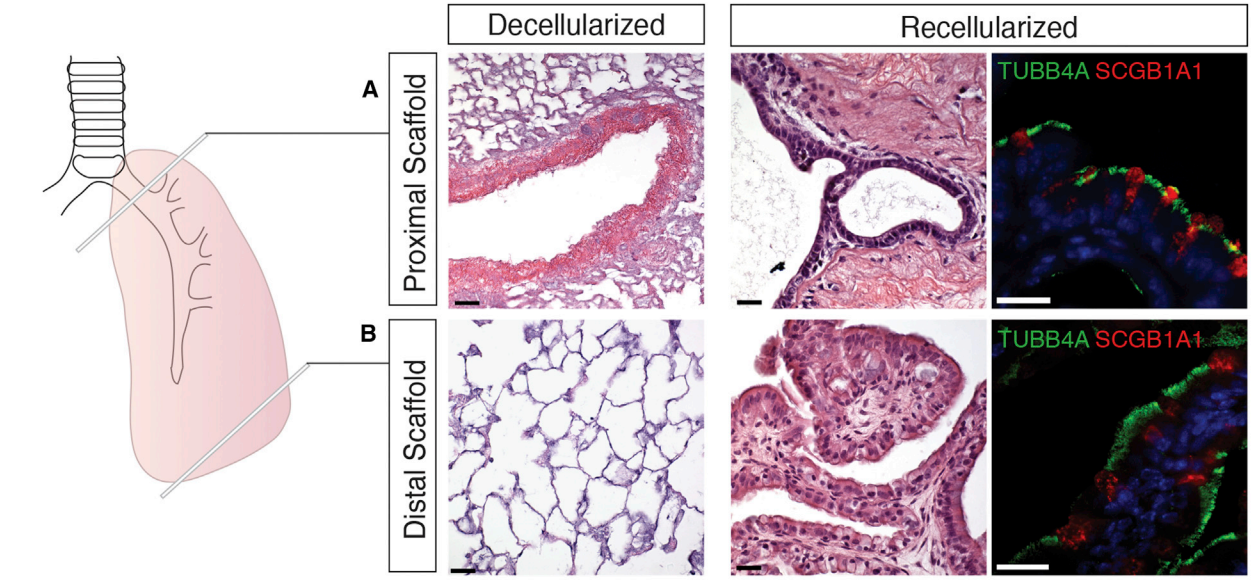

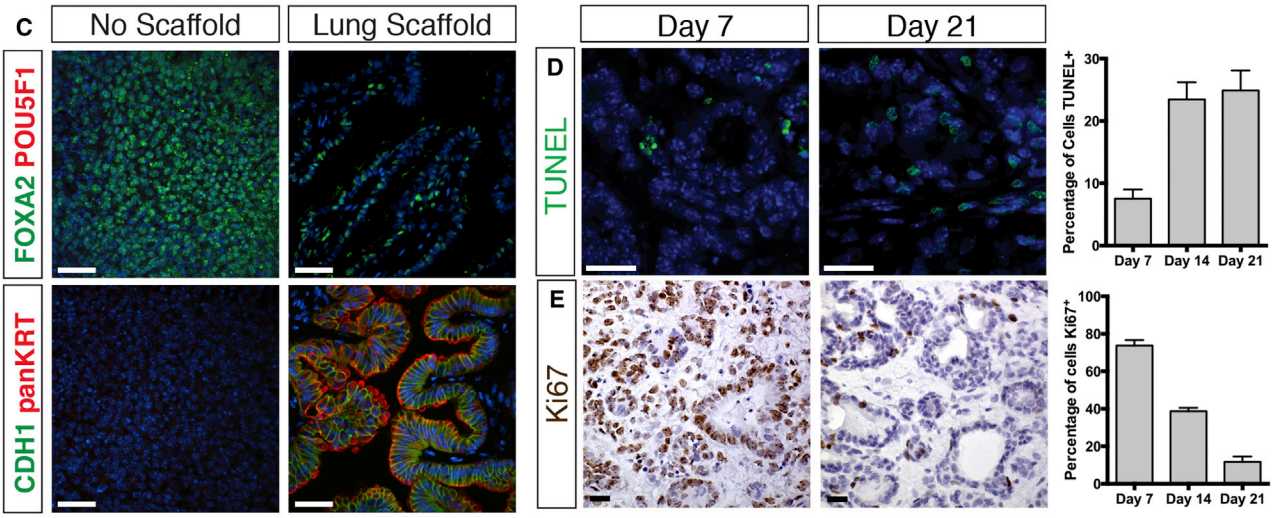

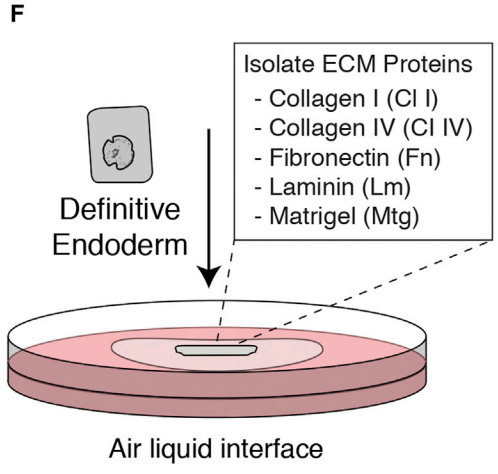

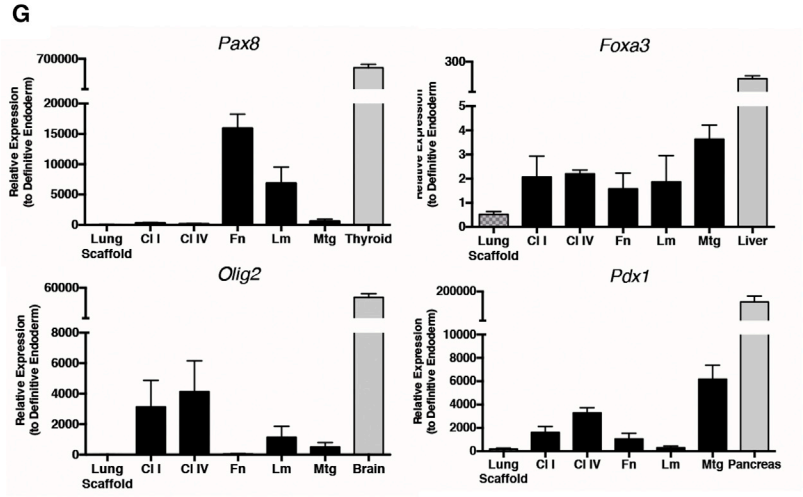

(legend on next page)

Mature differentiated epithelial sheets had established junctional complexes that were clearly identified with EM analysis (Figures 2F and 2I) and IF staining for tight junction-associated protein, TJP1 (Figure 4E). Stacked confocal images showed polarized cystic fibrosis transmembrane conductance regulator (CFTR) expression on the apical cell membranes, a characteristic feature of functional airway epithelial cells required for chloride and water transport in the airways (Figure 4F). CFTR channel activity was assessed using a cAMP-stimulated halide flux assay. Iodide efflux from scaffold cultures after cAMP agonist stimulation was measured periodically to assess channel activity. Differentiated day 21 cells showed peak iodide efflux within the first minute of CFTR channel stimulation, demonstrating robust expression of functional CFTR protein in the day 21 scaffold cultures (Figure 4G).

Organization and Differentiation of Endodermal Cells Is Dependent on Heparan Sulfate Proteoglycans and Its Bound Factors Remaining on Decellularized Lung Scaffolds

To better understand the ECM inductive signals present in decellularized lungs, we selectively cleaved and removed two major growth factor-binding matrix proteins, heparan sulfate (HS) and chondroitin sulfate (CS) (Shannon et al., 2003; Thompson et al., 2007, 2010; Toriyama et al., 1997). Decellularized scaffolds were subjected to enzymatic degradation with heparitinase I or chondroitinase ABC to selectively cleave HS or CS and release any bound factors. Tomato-lectin immunostaining of scaffolds and spectral UV analysis of incubation solution after heparitinase treatment confirmed HS cleavage (Figures S5A and S5B), while immunoblot analysis of chondroitinase ABC-treated scaffolds confirmed CS cleavage (data not shown). Basement membrane proteins laminin and collagen IV were preserved with both treatments (Figures S5C and S5D). Enzyme-treated scaffolds were seeded with definitive endoderm and cultured under ALI conditions as before for up to 21 days.

Scaffolds treated with chondroitinase-ABC did not show a significant difference in promoting lung-lineage differentiation of endodermal cells, while treatment with heparitinase I resulted in a complete loss of organization and differentiation (Figure 5A). SEM analysis showed a lack of epithelial morphology and tight junction coupling of seeded cells in heparitinase I-treated scaffolds (Figure 5B).

Using a commercially available proteome profiler antibody array, we detected 31 proteins from the array profile that remained on lung scaffolds after decellularization (Figure 5C). As an initial screen, a comparison of the protein profile from scaffolds treated with or without heparitinase I identified several candidate HS-bound proteins that were removed and found in the wash supernatant after enzyme treatment: CXCL12, serpinE1, PDGF-AB, HGF, MMP8, FGF2, proliferin, IL10, and CCL3 (Figure 5C). This revealed that ECM-inductive cues essential for organization and lung-lineage differentiation are dependent on HS proteoglycans and factors that may be bound to HS on decellularized scaffolds.

DISCUSSION

Lineage restriction of pluripotent cells is dependent on the interaction of niche components in the microenvironment, where growth-factor signaling, cell-cell contact, and cell-matrix interactions combine and control stem cell fate.

Figure 3. Proximal and Distal Lung Scaffolds Both Promote Airway Differentiation, while Isolate Matrix Proteins Alone Do Not Support Lung Lineage Commitment of Seeded Endodermal Cells

(A and B) Decellularized sections from both the proximal and distal regions of the lungs were generated and seeded with sorted endodermal cells. Tissue and IF staining show that both matrix sources promoted differentiation to airway ciliated (TUBB4A) and club (SCGB1A1) cells. Scale bars represent 25 μm.

(C) Immunostaining analysis demonstrates that endodermal cells seeded on lung scaffolds maintain definitive endoderm marker FOXA2 and do not express pluripotency marker POU5F1. Luminal structures are positive for epithelial cell markers CDH1 and panKRT. In contrast to cells seeded on scaffolds, endodermal cells cultured at ALI without the support of the lung matrix do not form organized structures and do not express epithelial cell markers. Scale bar represents 25 μm.

(D) TUNEL staining for identification of apoptotic cells on tissue sections was completed for different time points. Cell counts of immunostained sections shows the percentage of apoptotic ($TUNEL^+$) cells at days 7, 14, and 21 cultures. Scale bars represent 25 μm. Mean ± SEM, n = 3 experiments.

(E) Immunostaining for Ki67 shows a decline in proliferation with progressive differentiation of seeded cells to airway epithelia from day 7 to day 21 (scale bar represents 25 μm); mean ± SEM, n = 3 experiments.

(F) Schematic representation of isolated matrix-protein recellularization. Sorted endodermal cells are seeded on specific matrix proteins or Matrigel and cultured at ALI in base supportive media.

(G) Real-time PCR analysis reveals upregulation of other endodermal lineage (*Pax8*, *Foxa3*, *Pdx1*) and neuroectoderm (*Olig2*) markers with culture of definitive endoderm on isolated matrix proteins compared with lung scaffolds. Gene expression is presented relative to definitive endoderm; mean ± SEM, n = 3 experiments.

See also Figures S3 and S4.

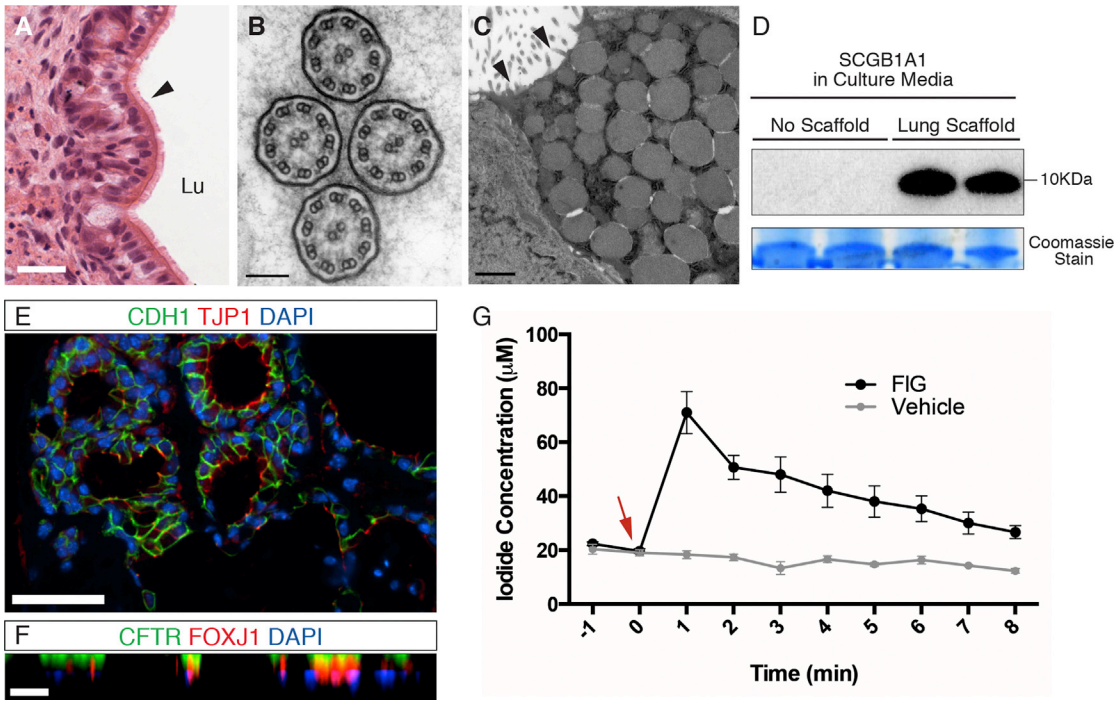

Figure 4. Differentiated Airway Epithelial Cultures Consist of Mature Airway Epithelia with Functional CFTR Protein

(A) H&E staining of day 21 scaffold cultures shows a sheet of ciliated cells lining a luminal structure. Scale bar represents 25 μm.

(B) Transmission EM image of cilia shows formation of the appropriate 9+2 dynein arms of motile respiratory cilia. Scale bar represents 100 nm.

(C) Transmission EM of day 21 cultures shows characteristic secretory vesicles inside differentiated club cells with microvilli lining the cell surface (black arrowheads). Scale bar represents 1 μm.

(D) Western blot of d21 culture media shows secreted SCGB1A1, while it is not detected in endodermal cultures without the lung scaffold. Coomassie stain is used as loading control; presented band is at 55 kDa.

(E) IF staining of cell cultures shows mature epithelial sheets with established tight junctions, represented by positive TJP1 staining of $CDH1^+$ epithelial cells. Scale bar represents 50 μm.

(F) Stacked confocal images (X-Z plane) show polarized CFTR expression on the apical cell membranes. Scale bar represents 25 μm.

(G) Iodide flux was measured after cAMP agonist-induced CFTR activity in day 21 scaffold cultures. cAMP agonists, forskolin and 3-isobutyl-1-methylxanthine, and a CFTR potentiator, genistein (together as forskolin, 3-isobutyl-1-methylxanthine [IBMX], and genistein) (FIG), were added (0 min, red arrow) and replaced periodically for 8 minutes while iodide flux was measured every minute. Peak efflux, 70.6 ± 7.7 μM, was reached immediately with addition of FIG at 1 min. No efflux was detected with added vehicle control (DMSO). n = 3 experiments; mean ± SEM.

See also Movie S1.

Growth factors are a salient component of directing cellular identity, and the ECM plays an important role in controlling growth factor availability by often binding and regulating local concentrations in space and time (Alberti et al., 2008; Discher et al., 2009; Murry and Keller, 2008; Peerani et al., 2007; Thompson et al., 2010). Because of the complex nature of these interactions during lung development, in vitro differentiation of PSC to functional airway epithelial cell populations remains a challenging task.

Here we report the robust differentiation of embryonic stem cell-derived endoderm to mature, functional airway epithelial cells using defined, serum-free culture on decellularized lung scaffolds at air liquid interface. Decellularized scaffolds alone directed differentiation of definitive endoderm to primarily $NKX2\text{-}1^+/SOX2^+/TRP63^+$ lung progenitor cells as early as 7 days of culture. This progenitor population expanded with longer duration and formed fully differentiated airway luminal structures with basal cells, club cells, and beating ciliated cells. This was achieved with notable morphological and functional resemblance to native airway epithelia, providing a 3D in vitro platform to better understand cell-matrix signaling during lung development and an efficient approach for generating mature airway epithelia from PSC. Although few $NKX2\text{-}1^+/SOX9^+$ cells were detected after 7 days of culture, they disappeared with longer duration of culture, suggesting that differentiation to the distal lineage requires additional inductive factors after $NKX2\text{-}1^+$ specification on scaffolds.

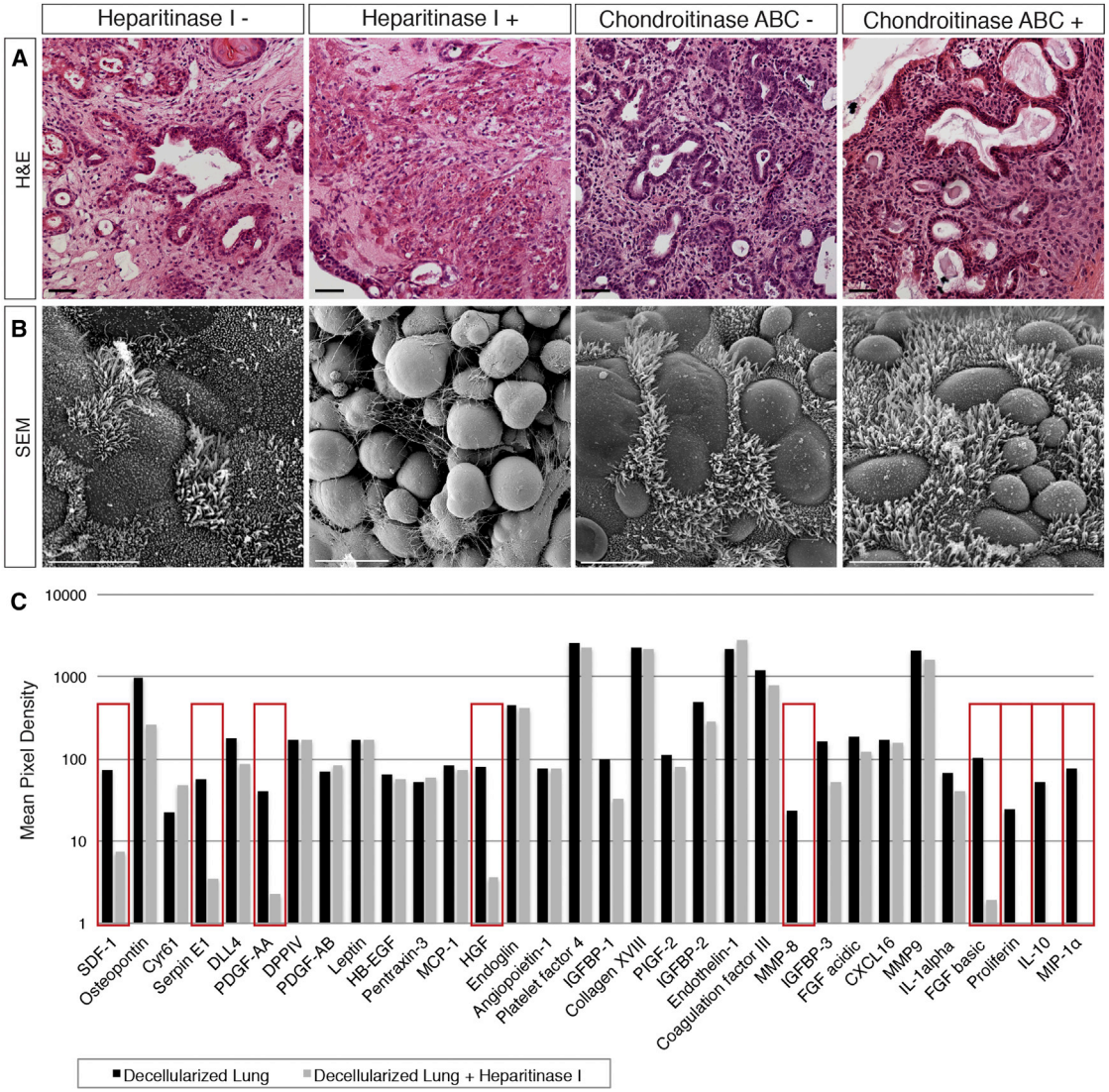

Figure 5. Organization and Differentiation of Endodermal Cells is Dependent on HS Proteoglycans on Decellularized Lung Scaffolds

(A) Acellular scaffolds were recellularized after heparitinase I or chondroitinase ABC treatment. H&E staining of day 21 seeded scaffold cultures show limited organization and differentiation in the heparitinase I-treated group, while chondroitinase ABC-treated cultures resemble control groups. Scale bar represents 50 μm.

(B) Scanning EM analysis of cultures show a lack of epithelial morphology and tight junction coupling of seeded cells in heparitinase I-treated scaffolds, where cells appear rounded with no resemblance to a lung phenotype. Scale bar represents 10 μm.

(C) Proteome profiler antibody array detects 31 proteins from the array profile that are remaining on lung scaffolds (black). Comparison of the protein profile from decellularized scaffolds treated with or without heparitinase I revealed several HS-bound proteins that are removed from scaffolds and found in the wash supernatant after enzyme treatment (red rectangles): CXCL12, serpinE1, PDGF-AB, HGF, MMP8, FGF2, proliferin, IL10, and CCL3. Data presented are average of two arrays from separate experiments.

See also Figure S5.

Recent reports have had success with promoting differentiation of PSC first to NKX2-1^{+} lung progenitor cells and further to airway (Gilpin et al., 2014; Gouon-Evans et al., 2006; Huang et al., 2014; Kubo et al., 2004; Mou et al., 2012; Wong et al., 2012) or alveolar (Ghaedi et al., 2013; Huang et al., 2014; Jensen et al., 2012; Kimura et al., 1996; Longmire et al., 2012; Minoo et al., 1999) epithelial cells using monolayer cultures and supplementation with inductive factors. However, these monolayer protocols achieved lung differentiation to a limited repertoire of functional epithelial cells with unclear efficiencies, potential contamination from other endodermal lineages,

lacking relevant 3D structure and in some cases with undefined culture conditions using fetal bovine serum. To our knowledge, there have been no previous reports demonstrating the efficient generation of stem cell-derived mature airway structures with CFTR function differentiated with extended culture on decellularized lung scaffolds alone.

The ability to repopulate decellularized scaffolds in culture has been used as an assay to assess the regenerative potential of differentiated cells in previous reports, where primary cells or predifferentiated cells derived from PSC have been seeded onto rat or human decellularized lungs (Bilodeau et al., 2014; Ghaedi et al., 2013; Gilpin et al., 2014; Huang et al., 2014; Jensen et al., 2012; Longmire et al., 2012; Ott et al., 2010; Petersen et al., 2010). Successful repopulation and maturation of seeded cells on lung scaffolds achieved by these studies reinforces the importance of a 3D ECM setting for supporting cell adherence, organization, and maturation. However, in these models, cells were seeded after specification to the lung lineage using inductive factors in monolayer cultures, and supplementation continued after seeding on scaffolds, therefore hindering assessment of the influence of lung ECM solely on promoting lineage-specific differentiation.

Interestingly, this distinct ability of decellularized lung to differentiate endoderm into airway epithelia was further restated by the lack of differentiation achieved with seeded isolated matrix proteins (fibronectin, laminin, collagen I, collagen IV), ECM substitute Matrigel, and decellularized kidney scaffolds. Differentiation on lung scaffolds was replicated using mouse-derived lung scaffolds and rat-derived ES cells. This demonstrates the conserved nature of this interaction between mouse and rat lung scaffolds with cell lines derived from both species.

Matrix-associated HS and CS proteoglycans are major modulators of growth factor binding and signaling on the ECM surface and function by stabilizing FGF/FGFR complexes, increasing local gradients, and promoting FGF internalization and processing (Izvolsky et al., 2003; Kimura and Deutsch, 2007; Shannon et al., 2003; Thompson et al., 2010). Specification to the airway lineage in our model was found to be dependent on HS proteoglycans and bound factors remaining on scaffolds. Using a proteome profiler antibody array as an initial screen, we showed that numerous proteins remain on scaffolds after decellularization. A list of potential candidates implicated in lung specification was identified using this method, although the array profile is not an exhaustive list and a more in-depth analysis is required to parse out the HS-bound proteins present on scaffolds that are essential for differentiation.

Given the role of the ECM in integrating and mediating inductive signals in a 3D setting and our success with the efficient differentiation of embryonic stem cell-derived endodermal cells to functional airway epithelia, decellularized lung scaffolds are an attractive in vitro platform for lung airway engineering. This differentiation strategy generates a renewable source of functional airway epithelial cells in a 3D matrix setting that can be further examined for regenerative potential in vivo. Seeded decellularized lung scaffolds from human or xenogeneic sources can be used for generation of lung epithelia that may be valuable for airway repair and regeneration and can serve as a platform for drug discovery in human airway-related diseases such as cystic fibrosis.

EXPERIMENTAL PROCEDURES

ESC Culture and Endoderm Induction

Mouse ESC lines (R1 (*Nkx2-1*^{mCherry}) (Bilodeau et al., 2014; Perl et al., 2005; Que et al., 2009), G4 (*dsRed-MST*), and129/Ola (*Bry-GFP*/*Foxa2-hCD4*), and rat ESC line (*DAc8*) were maintained in the pluripotent state under feeder-free, serum-free culture using 2i media conditions (Hong et al., 2004; Rock et al., 2009; Ying et al., 2008). Endoderm induction was achieved in serum-free differentiation media (SFDM) supplemented with activin A (El-Gawad and Westfall, 2000; Gouon-Evans et al., 2006; Peão et al., 1993). Cells were sorted for dual expression of definitive endoderm markers cKIT and CXCR4 after induction. A detailed protocol is provided in the Supplemental Experimental Procedures.

Decellularization and Recellularization

Animal husbandry and procedures were approved and carried out in accordance with the Animal Care Committee guidelines of the Hospital for Sick Children. Mouse and rat lungs were decellularized using a CHAPS-based decellularization solution followed by a rapid wash and decontamination protocol to remove cellular material. Thick sections (350 μM) of lung scaffolds were generated using a vibratome and placed on hydrophobic floating membranes in culture (Whatman #110614) to achieve ALI culture conditions. Scaffolds were seeded with 100,000 sorted definitive endoderm cells (cKIT$^+$/CXCR4$^+$) and maintained for up to 21 days using SFDM, with no additional growth factor supplementation. Details of the procedure are outlined in the Supplemental Experimental Procedures.

Characterization of Decellularized Scaffolds

Removal of cellular material from decellularized lungs was confirmed using tissue staining, EM, and DNA assay analysis. Preservation of matrix proteins and properties was confirmed using IF staining for matrix proteins, Hart's elastin stain, immunoblot analysis, immuno-TEM, and tensile strength testing. Detailed protocols for scaffold characterization are outlined in the Supplemental Experimental Procedures.

qPCR

Quantitative amplification of template cDNA was done using SYBR GreenER qPCR SuperMix (Life Technologies). Gene expression was normalized to RNA Polymerase II and expressed relative to selected positive (adult tissue, E13 lung) or negative controls (definitive endoderm). Details of the protocol are outlined in the Supplemental Experimental Procedures.

Immunostaining

Seeded scaffold cultures were fixed with 4% paraformaldehyde, paraffin embedded, and sectioned at 5 μm. Sample sections were rehydrated, and heat-induced epitope retrieval with citrate buffer was performed. Slides were then blocked for 1 hr with 5% normal donkey serum and 1% BSA in PBS for 1 hr at room temperature. Samples were then incubated with primary antibodies at 4°C overnight in a humidified chamber and detected using appropriate secondary antibodies (Invitrogen) for 1 hr at room temperature. For immunofluorescence, nuclei were counterstained using 4′,6-diamidino-2-phenylindole (Invitrogen). Details of antibodies and imaging are provided in the Supplemental Experimental Procedures.

EM

Samples were fixed in 2.5% gluteraldehyde in 0.1 M phosphate buffer (pH 7.4). Sample processing and microscopy details are described in the Supplemental Experimental Procedures.

Iodide Flux Assay

CFTR channel activity was assessed using a cAMP-stimulated halide flux assay to measure iodide flux across the apical membrane of day 21 differentiated epithelial cultures. Details of the assay are provided in the Supplemental Experimental Procedures.

Scaffold Enzymatic Treatment

HS or CS proteoglycans were cleaved from decellularized lung scaffolds using treatment with heparitinase I (Amsbio #100704) or chondroitinase ABC (Amsbio #100330-1A), respectively. Details of the enzymatic treatment are provided in the Supplemental Experimental Procedures.

Protein Profiler Array

A protein antibody array (R&D Systems, ARY015) was used to identify candidate proteins remaining on decellularized scaffolds with or without heparitinase I treatment, as per manufacturer's instructions. Details of the array protocol are provided in the Supplemental Experimental Procedures.

Statistical Analysis

Statistical comparisons were performed using unpaired t tests, unless specified otherwise. For multiple comparisons of more than two groups, one-way ANOVA was used with Dunnett's test for significance.

SUPPLEMENTAL INFORMATION

Supplemental Information includes Supplemental Experimental Procedures, five figures, and one movie and can be found with this article online at http://dx.doi.org/10.1016/j.stemcr.2015.01.004.

Received: September 23, 2014
Revised: January 6, 2015
Accepted: January 8, 2015
Published: February 5, 2015

REFERENCES

Alberti, K., Davey, R.E., Onishi, K., George, S., Salchert, K., Seib, F.P., Bornhäuser, M., Pompe, T., Nagy, A., Werner, C., and Zandstra, P.W. (2008). Functional immobilization of signaling proteins enables control of stem cell fate. Nat. Methods *5*, 645–650.

Bilodeau, M., Shojaie, S., Ackerley, C., Post, M., and Rossant, J. (2014). Identification of a proximal progenitor population from murine fetal lungs with clonogenic and multilineage differentiation potential. Stem Cell Rep. *3*, 634–649.

Daley, W.P., Peters, S.B., and Larsen, M. (2008). Extracellular matrix dynamics in development and regenerative medicine. J. Cell Sci. *121*, 255–264.

Discher, D.E., Mooney, D.J., and Zandstra, P.W. (2009). Growth factors, matrices, and forces combine and control stem cells. Science *324*, 1673–1677.

El-Gawad, M.A., and Westfall, J.A. (2000). Comparative ultrastructure of Clara cells in neonatal and older cattle. J. Morphol. *244*, 143–151.

Engelhardt, J.F., Schlossberg, H., Yankaskas, J.R., and Dudus, L. (1995). Progenitor cells of the adult human airway involved in submucosal gland development. Development *121*, 2031–2046.

Ghaedi, M., Calle, E.A., Mendez, J.J., Gard, A.L., Balestrini, J., Booth, A., Bove, P.F., Gui, L., White, E.S., and Niklason, L.E. (2013). Human iPS cell-derived alveolar epithelium repopulates lung extracellular matrix. J. Clin. Invest. *123*, 4950–4962.

Gilpin, S.E., Ren, X., Okamoto, T., Guyette, J.P., Mou, H., Rajagopal, J., Mathisen, D.J., Vacanti, J.P., and Ott, H.C. (2014). Enhanced lung epithelial specification of human induced pluripotent stem cells on decellularized lung matrix. Ann. Thorac. Surg. *98*, 1721–1729.

Gouon-Evans, V., Boussemart, L., Gadue, P., Nierhoff, D., Koehler, C.I., Kubo, A., Shafritz, D.A., and Keller, G. (2006). BMP-4 is required for hepatic specification of mouse embryonic stem cell-derived definitive endoderm. Nat. Biotechnol. *24*, 1402–1411.

Green, M.D., Chen, A., Nostro, M.-C., d'Souza, S.L., Schaniel, C., Lemischka, I.R., Gouon-Evans, V., Keller, G., and Snoeck, H.-W. (2011). Generation of anterior foregut endoderm from human embryonic and induced pluripotent stem cells. Nat. Biotechnol. *29*, 267–272.

Hong, K.U., Reynolds, S.D., Watkins, S., Fuchs, E., and Stripp, B.R. (2004). In vivo differentiation potential of tracheal basal cells: evidence for multipotent and unipotent subpopulations. Am. J. Physiol. Lung Cell. Mol. Physiol. *286*, L643–L649.

Huang, S.X.L., Islam, M.N., O'Neill, J., Hu, Z., Yang, Y.-G., Chen, Y.-W., Mumau, M., Green, M.D., Vunjak-Novakovic, G., Bhattacharya, J., and Snoeck, H.W. (2014). Efficient generation of lung and airway epithelial cells from human pluripotent stem cells. Nat. Biotechnol. *32*, 84–91.

Izvolsky, K.I., Shoykhet, D., Yang, Y., Yu, Q., Nugent, M.A., and Cardoso, W.V. (2003). Heparan sulfate-FGF10 interactions during lung morphogenesis. Dev. Biol. *258*, 185–200.

Jensen, T., Roszell, B., Zang, F., Girard, E., Matson, A., Thrall, R., Jaworski, D.M., Hatton, C., Weiss, D.J., and Finck, C. (2012). A rapid lung de-cellularization protocol supports embryonic stem cell

differentiation in vitro and following implantation. Tissue Eng. Part C Methods *18*, 632–646.

Kimura, J., and Deutsch, G.H. (2007). Key mechanisms of early lung development. Pediatr. Dev. Pathol. *10*, 335–347.

Kimura, S., Hara, Y., Pineau, T., Fernandez-Salguero, P., Fox, C.H., Ward, J.M., and Gonzalez, F.J. (1996). The T/ebp null mouse: thyroid-specific enhancer-binding protein is essential for the organogenesis of the thyroid, lung, ventral forebrain, and pituitary. Genes Dev. *10*, 60–69.

Kubo, A., Shinozaki, K., Shannon, J.M., Kouskoff, V., Kennedy, M., Woo, S., Fehling, H.J., and Keller, G. (2004). Development of definitive endoderm from embryonic stem cells in culture. Development *131*, 1651–1662.

Longmire, T.A., Ikonomou, L., Hawkins, F., Christodoulou, C., Cao, Y., Jean, J.C., Kwok, L.W., Mou, H., Rajagopal, J., Shen, S.S., et al. (2012). Efficient derivation of purified lung and thyroid progenitors from embryonic stem cells. Cell Stem Cell *10*, 398–411.

Minoo, P., Su, G., Drum, H., Bringas, P., and Kimura, S. (1999). Defects in tracheoesophageal and lung morphogenesis in Nkx2.1(-/-) mouse embryos. Dev. Biol. *209*, 60–71.

Mou, H., Zhao, R., Sherwood, R., Ahfeldt, T., Lapey, A., Wain, J., Sicilian, L., Izvolsky, K., Musunuru, K., Cowan, C., and Rajagopal, J. (2012). Generation of multipotent lung and airway progenitors from mouse ESCs and patient-specific cystic fibrosis iPSCs. Cell Stem Cell *10*, 385–397.

Murry, C.E., and Keller, G. (2008). Differentiation of embryonic stem cells to clinically relevant populations: lessons from embryonic development. Cell *132*, 661–680.

Ott, H.C., Clippinger, B., Conrad, C., Schuetz, C., Pomerantseva, I., Ikonomou, L., Kotton, D., and Vacanti, J.P. (2010). Regeneration and orthotopic transplantation of a bioartificial lung. Nat. Med. *16*, 927–933.

Peão, M.N., Aguas, A.P., de Sá, C.M., and Grande, N.R. (1993). Anatomy of Clara cell secretion: surface changes observed by scanning electron microscopy. J. Anat. *182*, 377–388.

Peerani, R., Rao, B.M., Bauwens, C., Yin, T., Wood, G.A., Nagy, A., Kumacheva, E., and Zandstra, P.W. (2007). Niche-mediated control of human embryonic stem cell self-renewal and differentiation. EMBO J. *26*, 4744–4755.

Perl, A.-K.T., Kist, R., Shan, Z., Scherer, G., and Whitsett, J.A. (2005). Normal lung development and function after Sox9 inactivation in the respiratory epithelium. Genesis *41*, 23–32.

Petersen, T.H., Calle, E.A., Zhao, L., Lee, E.J., Gui, L., Raredon, M.B., Gavrilov, K., Yi, T., Zhuang, Z.W., Breuer, C., et al. (2010). Tissue-engineered lungs for in vivo implantation. Science *329*, 538–541.

Que, J., Luo, X., Schwartz, R.J., and Hogan, B.L.M. (2009). Multiple roles for Sox2 in the developing and adult mouse trachea. Development *136*, 1899–1907.

Rock, J.R., Onaitis, M.W., Rawlins, E.L., Lu, Y., Clark, C.P., Xue, Y., Randell, S.H., and Hogan, B.L.M. (2009). Basal cells as stem cells of the mouse trachea and human airway epithelium. Proc. Natl. Acad. Sci. USA *106*, 12771–12775.

Shannon, J.M., McCormick-Shannon, K., Burhans, M.S., Shangguan, X., Srivastava, K., and Hyatt, B.A. (2003). Chondroitin sulfate proteoglycans are required for lung growth and morphogenesis *in vitro*. Am. J. Physiol. Lung Cell. Mol. Physiol. *285*, L1323–L1336.

Smolich, J.J., Stratford, B.F., Maloney, J.E., and Ritchie, B.C. (1978). New features in the development of the submucosal gland of the respiratory tract. J. Anat. *127*, 223–238.

Thompson, S.M., Connell, M.G., Fernig, D.G., Ten Dam, G.B., van Kuppevelt, T.H., Turnbull, J.E., Jesudason, E.C., and Losty, P.D. (2007). Novel 'phage display antibodies identify distinct heparan sulfate domains in developing mammalian lung. Pediatr. Surg. Int. *23*, 411–417.

Thompson, S.M., Jesudason, E.C., Turnbull, J.E., and Fernig, D.G. (2010). Heparan sulfate in lung morphogenesis: The elephant in the room. Birth Defects Res. C Embryo Today *90*, 32–44.

Toriyama, K., Muramatsu, H., Hoshino, T., Torii, S., and Muramatsu, T. (1997). Evaluation of heparin-binding growth factors in rescuing morphogenesis of heparitinase-treated mouse embryonic lung explants. Differentiation *61*, 161–167.

Wong, A.P., Bear, C.E., Chin, S., Pasceri, P., Thompson, T.O., Huan, L.-J., Ratjen, F., Ellis, J., and Rossant, J. (2012). Directed differentiation of human pluripotent stem cells into mature airway epithelia expressing functional CFTR protein. Nat. Biotechnol. *30*, 876–882.

Ying, Q.-L., Wray, J., Nichols, J., Batlle-Morera, L., Doble, B., Woodgett, J., Cohen, P., and Smith, A. (2008). The ground state of embryonic stem cell self-renewal. Nature *453*, 519–523.

Zorn, A.M., and Wells, J.M. (2009). Vertebrate endoderm development and organ formation. Annu. Rev. Cell Dev. Biol. *25*, 221–251.

Zuo, W., Zhang, T., Wu, D.Z., Guan, S.P., Liew, A., Yamamoto, Y., Wang, X., Lim, S.J., Vincent, M., Lessard, M., et al. (2014). p63(+) Krt5(+) distal airway stem cells are essential for lung regeneration. Nature. Published online November 12, 2014. http://dx.doi.org/10.1038/nature13903.

Stem Cell Reports

Supplemental Information

Acellular Lung Scaffolds Direct Differentiation of Endoderm to Functional Airway Epithelial Cells: Requirement of Matrix-Bound HS Proteoglycans

Sharareh Shojaie, Leonardo Ermini, Cameron Ackerley, Jinxia Wang, Stephanie Chin, Behzad Yeganeh, Mélanie Bilodeau, Manpreet Sambi, Ian Rogers, Janet Rossant, Christine E. Bear, and Martin Post

Figure S1

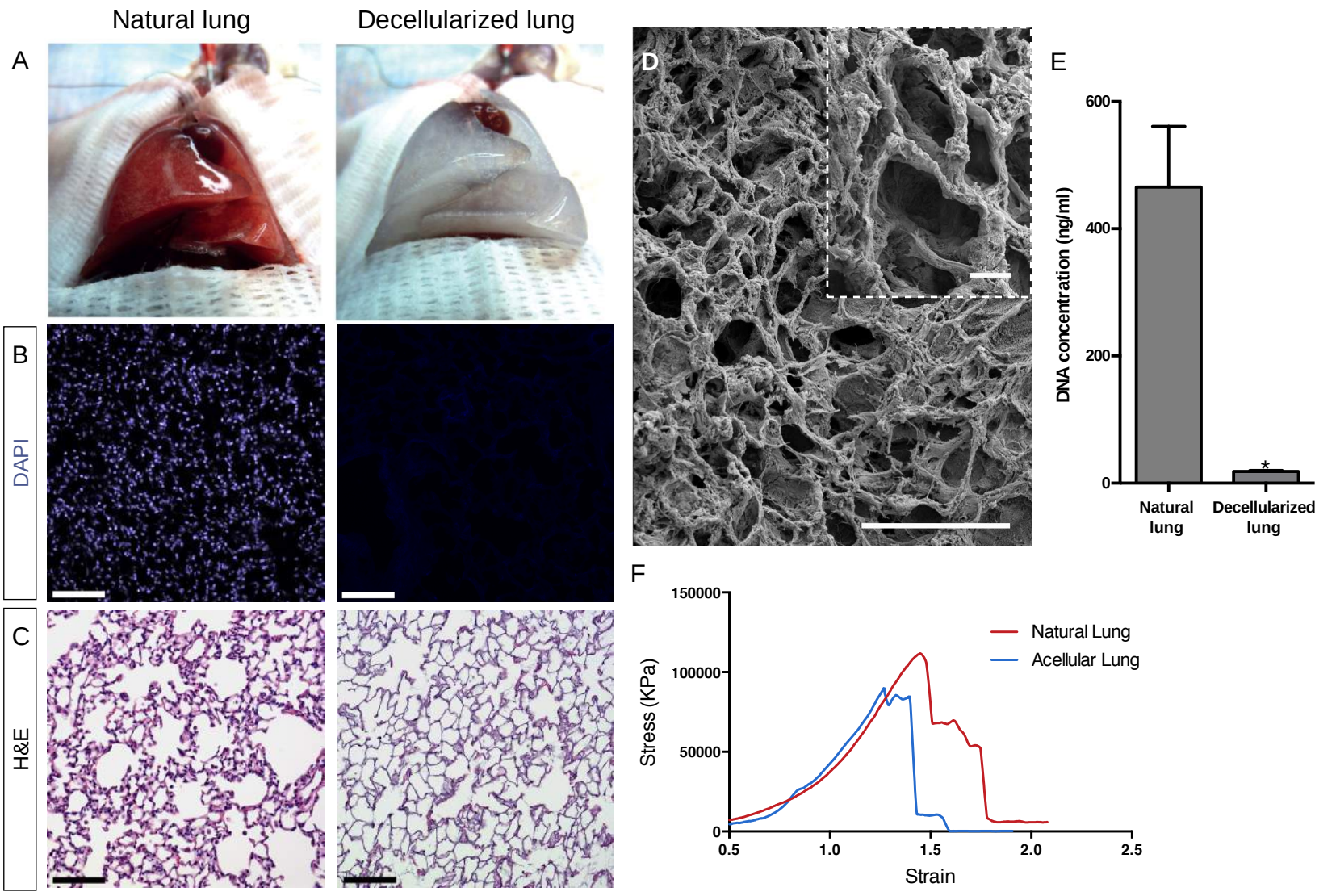
Natural lung
Decellularized lung
A
B
DAPI
C
H&E
D
E
DNA concentration (ng/ml)
600
400
200
0
*
Natural lung
Decellularized lung
F
Stress (KPa)
150000
100000
50000
0
0.5
1.0
1.5
2.0
2.5
Strain
Natural Lung
Acellular Lung
G
Col-I DAPI
Col-IV DAPI
Lmn DAPI
HSPG DAPI
Fn DAPI
Natural lung
Acellular lung
H
Elastin
I
Rinses post-decellularization
5 x
10 x
20 x
Natural lung
Laminin
268
238
Ponceau S
J

Figure S2

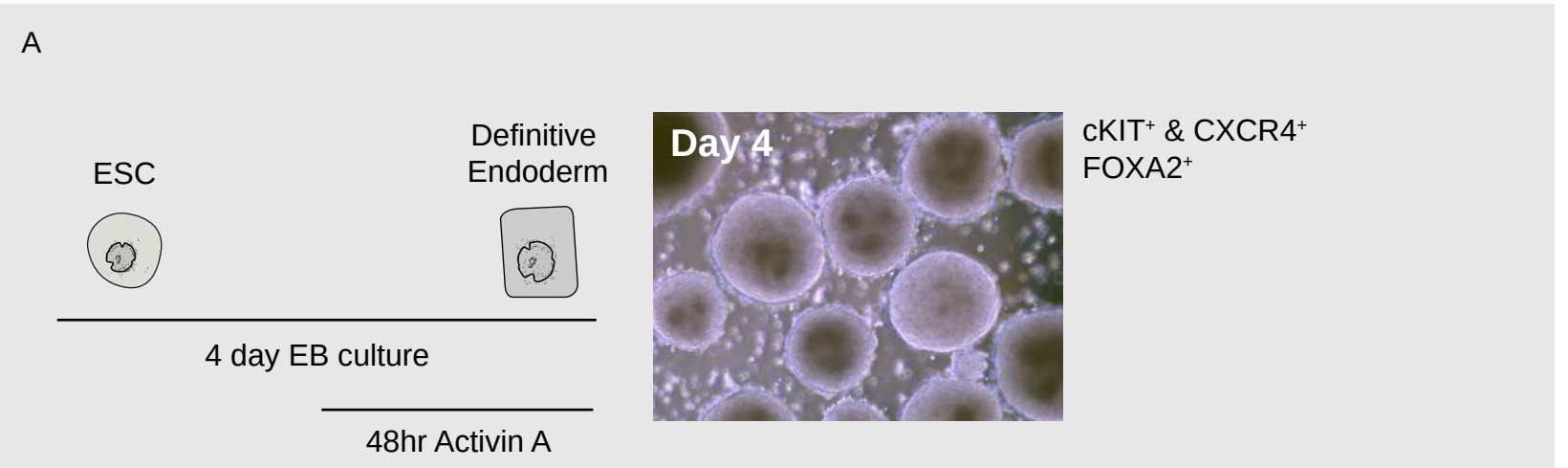
A
ESC
Definitive Endoderm
Day 4
cKIT+ & CXCR4+
FOXA2+
4 day EB culture
48hr Activin A

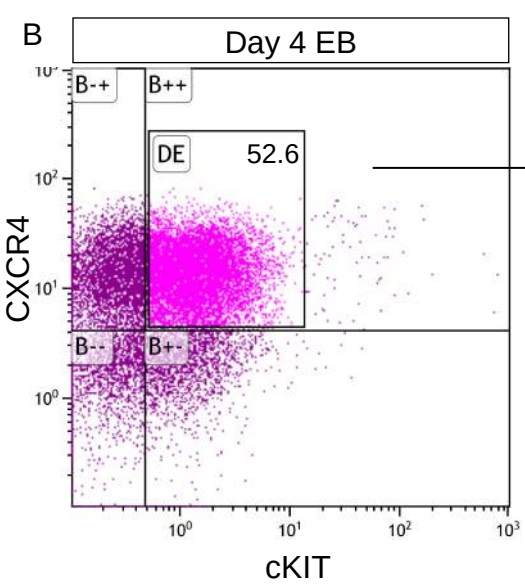
B
Day 4 EB
B-+
B++
DE
52.6
B--
B+-
CXCR4
cKIT

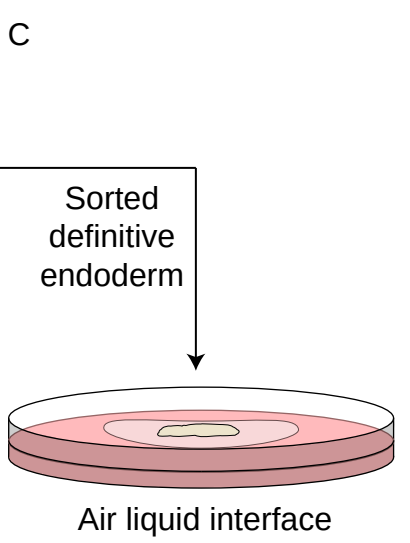
C
Sorted definitive endoderm
Air liquid interface

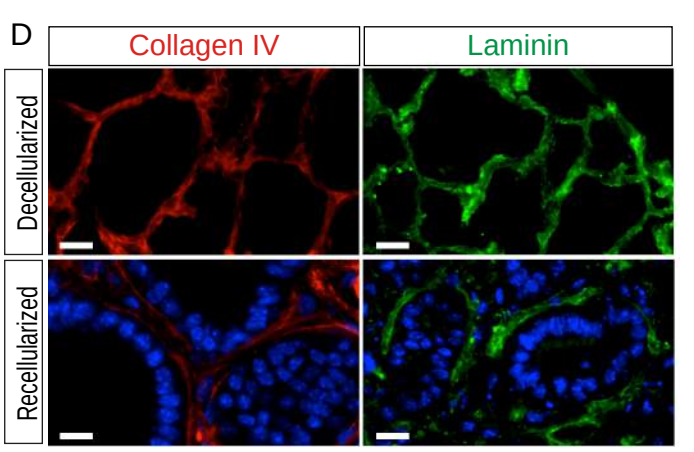
D
Collagen IV
Laminin
Decellularized
Recellularized

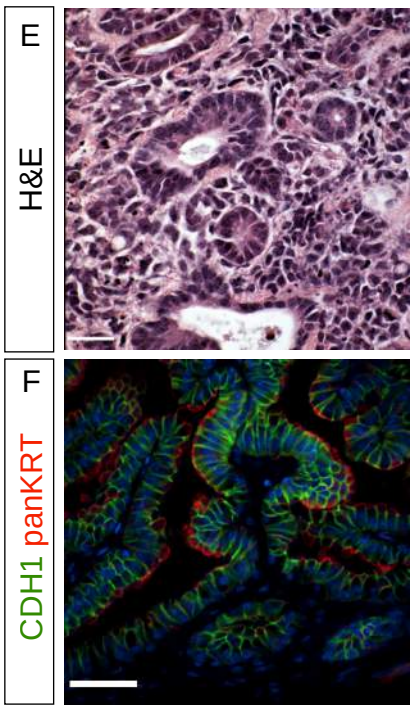
E
H&E
F
CDH1 panKRT

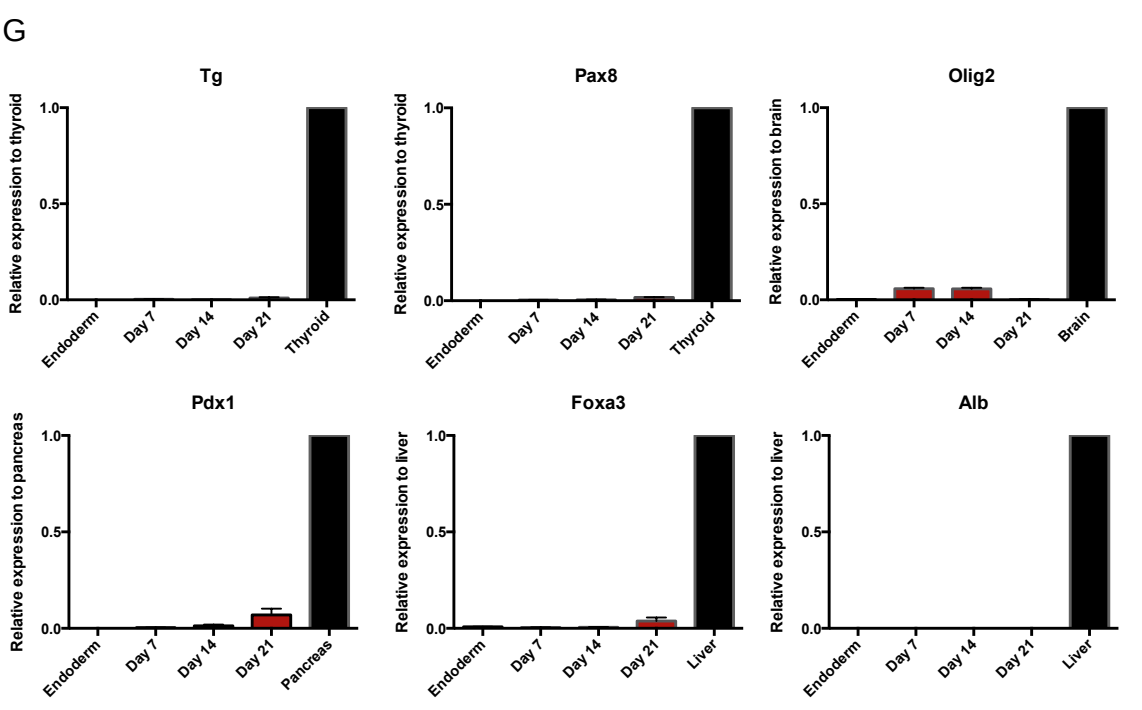
G
Tg
Pax8
Olig2
Pdx1
Foxa3
Alb
Relative expression to thyroid
Relative expression to brain
Relative expression to pancreas
Relative expression to liver
Endoderm
Day 7
Day 14
Day 21
Thyroid
Brain
Pancreas
Liver

Figure S3

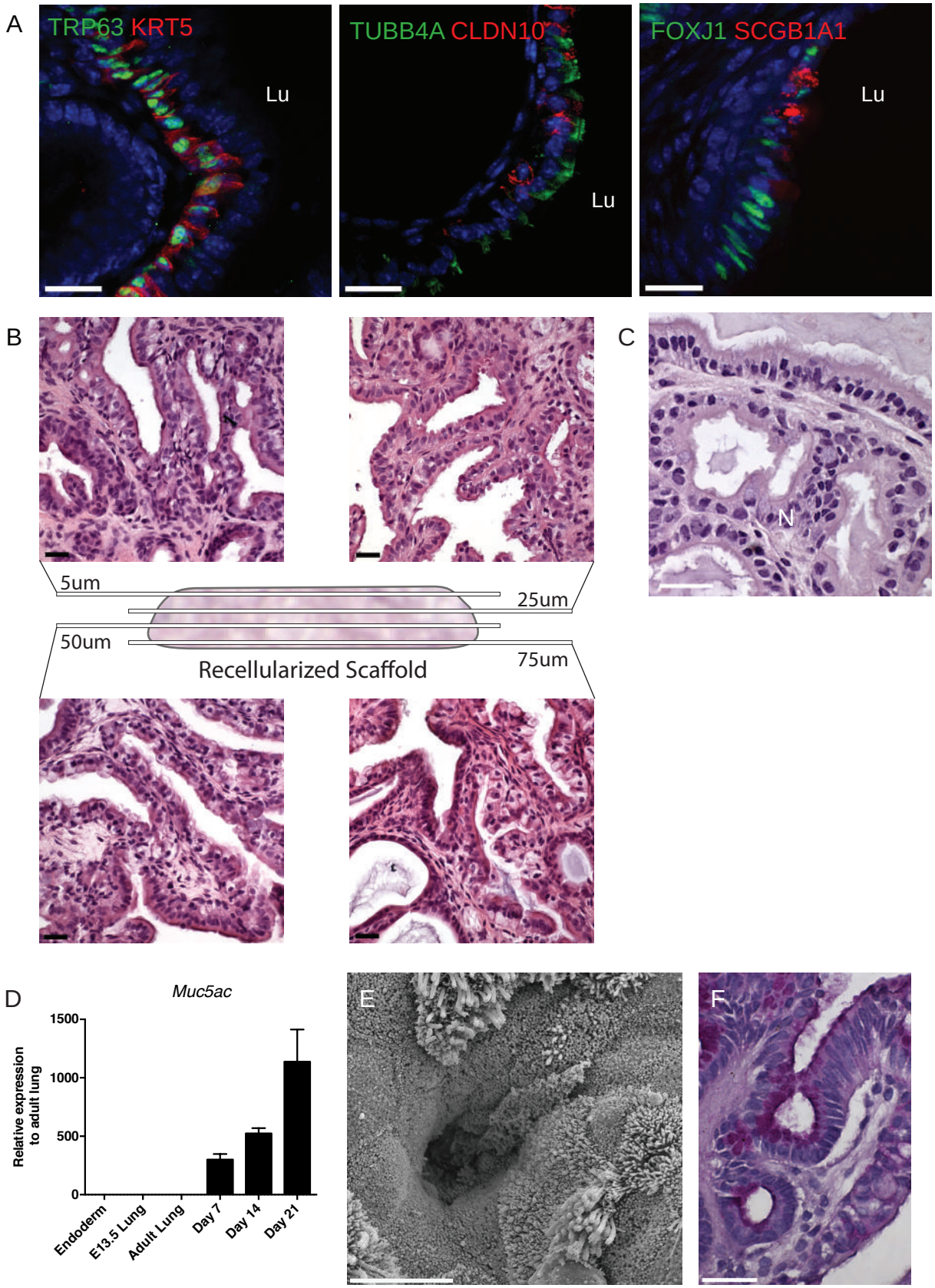
A
TRP63 KRT5
Lu
TUBB4A CLDN10
Lu
FOXJ1 SCGB1A1
Lu
B
5um
25um
50um
75um
Recellularized Scaffold
C
N
D
Muc5ac
Relative expression to adult lung
1500
1000
500
0
Endoderm
E13.5 Lung
Adult Lung
Day 7
Day 14
Day 21
E
F

Figure S4

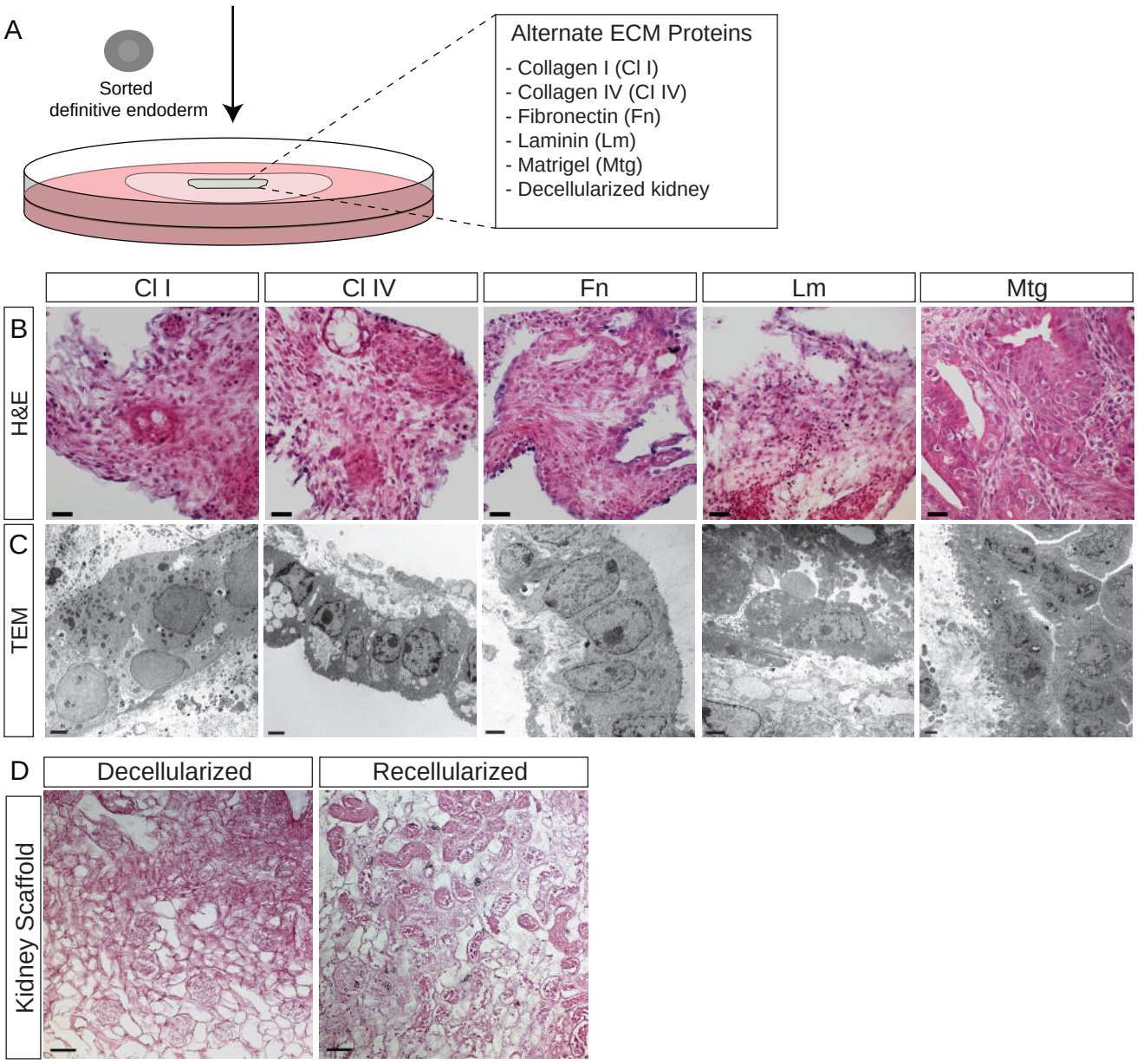
A
Sorted
definitive endoderm
Alternate ECM Proteins
- Collagen I (Cl I)
- Collagen IV (Cl IV)
- Fibronectin (Fn)
- Laminin (Lm)
- Matrigel (Mtg)
- Decellularized kidney
Cl I
Cl IV
Fn
Lm
Mtg
B
H&E
C
TEM
D
Decellularized
Recellularized
Kidney Scaffold

Figure S5

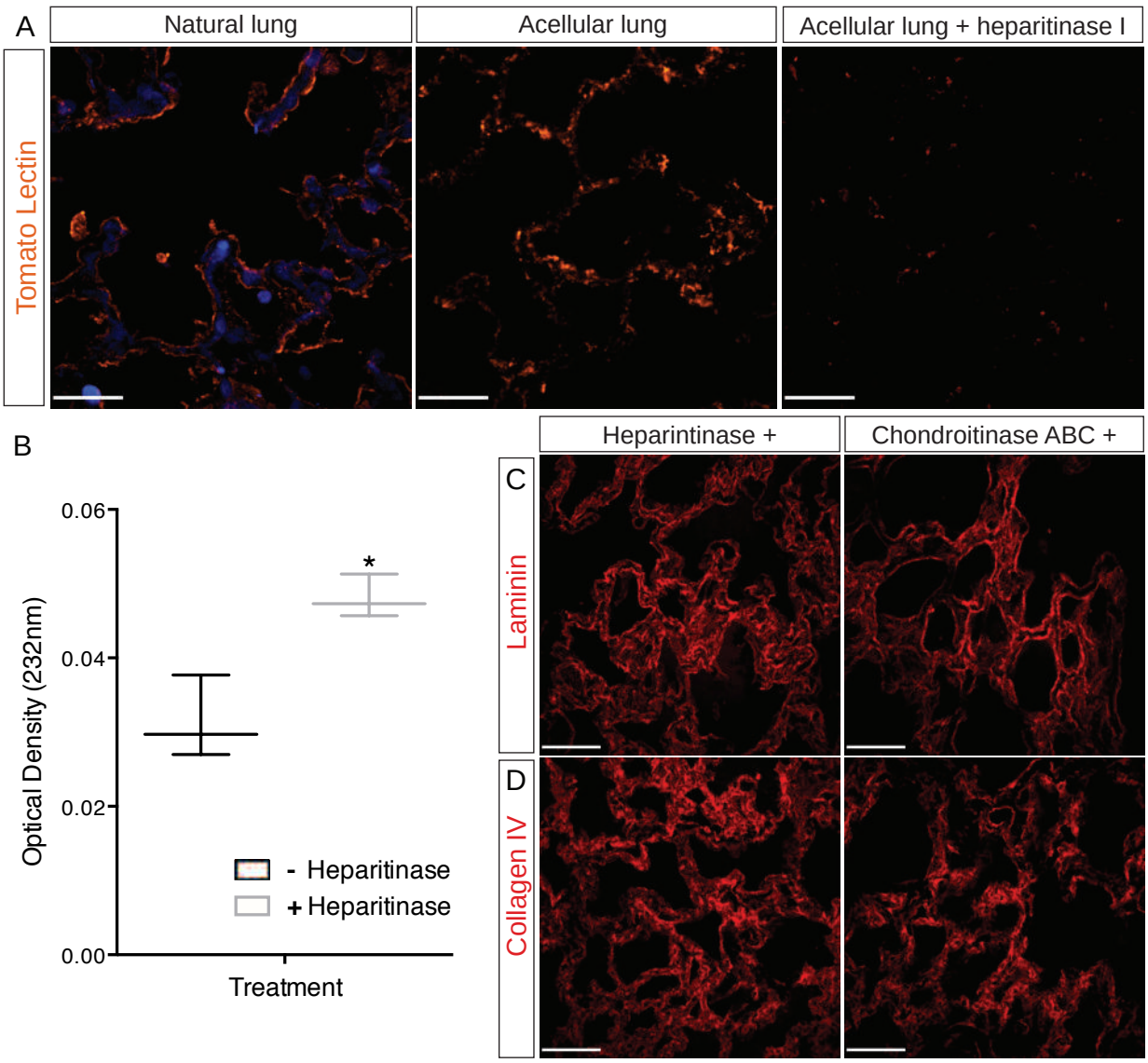
A
Natural lung
Acellular lung
Acellular lung + heparitinase I
Tomato Lectin
B
Optical Density (232nm)
0.06
0.04
0.02
0.00
*
- Heparitinase
+ Heparitinase
Treatment
Heparintinase +
Chondroitinase ABC +
C
Laminin
D
Collagen IV

Figure S1, Related to Figure 1. Decellularization of Adult Rat Lungs Removes Cellular Components While Maintaining Extracellular Matrix Structure and Protein Composition.

(A) Photographic representation of a natural lung (left panel) and an acellular lung (right panel) following decellularization with CHAPS-based solution. **(B-C)** Corresponding hematoxylin & eosin (H&E) and DAPI staining of natural and acellular lung tissue sections show the absence of cellular material including nuclei following decellularization. Scale bars=50µm. **(D)** Scanning electron microscope (EM) analysis following decellularization show the surface of acellular lung scaffolds with intact matrix architecture. Scale bar=100µm, scale bar of inset=10µm. **(E)** Removal of DNA following Benzonase treatment of decellularized scaffolds was confirmed with DNA assay. Mean ± SEM, n=3, *p<0.01. **(F)** Tensile testing represented by stress versus strain plots of natural and decellularized scaffolds characterize mechanical properties of scaffolds. Acellular scaffolds have a similar tensile strength curve profile, although with a lower overall peak strength, to natural lungs. **(G)** Natural (top panel) and acellular lungs (lower panel) were examined for ECM protein composition. Immunostaining analysis shows intact collagen I (Col-I), collagen IV (Col-IV), laminin (Lmn), heparan sulfate proteoglycans (HSPG), and fibronectin (Fn), while DAPI staining is absent from decellularized tissue. Scale bars =25µm. **(H)** Hart's elastin stain shows intact elastin fibers in scaffolds following decellularization. Scale bar=25µm. **(I)** Immunoblot analysis for basement membrane-protein laminin following 5, 10, and 20 washes after decellularization shows that scaffolds maintain laminin protein composition for up to 10 rinses. Ponceau stain was used as loading control, presented band is at 50kDa. **(J)** Transmission EM analysis shows decellularized scaffolds with positive immunogold staining for laminin (black arrowheads). Scale bar=500nm.

Figure S2, Related to Figure 1 and Figure 2. Decellularized Lung Scaffolds are Repopulated with ES-derived Definitive Endoderm Cells and Maintained at Air Liquid Interface.

(A) Definitive endoderm induction ($FOXA2^+$, $cKIT^+$ & $CXCR4^+$) is achieved with 48hr treatment of ES-derived embryoid bodies with 50ng/ml of Activin A. **(B)** Endodermal

cells are sorted for cKIT and CXCR4 using fluorescence-activated cell sorting to obtain an enriched population for recellularization. **(C)** Schematic representation of recellularization setup. Sorted definitive endoderm cells are seeded on thick sections (300-400µm) of acellular lung scaffold and cultured on a floating hydrophobic polycarbonate membrane to achieve an air-liquid interface, in serum- and growth factor-free supportive media. **(D)** Seeded endodermal cells repopulate scaffolds and organize into luminal structures. Immunostaining for collagen IV and laminin shows that these scaffold proteins line the developing cellular (DAPI positive) structures. **(E)** H&E staining of scaffold cultures reveals organization of seeded endodermal cells into luminal structures (day 7). Scale bar=50µm. **(F)** Positive immunostaining for panKRT and CDH1 reveals presence of epithelial cells. Scale bar=50µm. **(G)** Real time-PCR analysis shows that relative to expression of adult tissue (mean ± SEM, n=4 experiments), thyroid lineage makers *Tg* and *Pax8*, and neuroectoderm marker *Olig2* are hardly detected in seeded scaffolds after 7, 14, and 21 days of culture. Expression of additional endoderm lineage markers including *Pdx1* (pancreas), *Foxa3* (posterior endoderm), and *Albumin* (liver) are also marginally detected.

Figure S3, Related to Figure 2 and Figure 3. Prolonged Culture of Mouse- or Rat-derived Endoderm on Lung Scaffolds Promotes Differentiation to Airway Epithelial Cells

(A) Immunostaining of day 21 cultures for airway lineage markers shows the presence of basal cells ($TRP63^+$, $KRT5^+$) (left image), ciliated cells and club cells [$TUBB4A^+$, $CLDN10^+$ (center image), and $FOXJ1^+$, $SCGB1A1^+$ (right image)]. Scale bars=25µm. **(B)** Hematoxylin and eosin staining of day 21 tissue sections generated from various depths shows repopulation of entire decellularized scaffolds. **(C)** Decellularized rat scaffolds support repopulation and differentiation of Rat ESC (DAc8 cell line)-derived definitive endoderm to airway epithelial cells, similar to that achieved with mouse ESC lines. Scale bar=50µm. **(D)** RT-PCR analysis reveals upregulation of secretory cell marker *Muc5ac* in seeded cells with extended culture. Gene expression is presented relative to adult lung; mean ± SEM, n=3 experiments. **(E)** Scanning EM analysis reveals the presence of pit structures with ciliated and secretory cells lining the orifice. Scale

bar=5µm. **(F)** Pit structures present on epithelial surfaces show a strong PAS positive stain suggestive of mucin-producing cells lining these structures. Scale bar=50µm.

Figure S4, Related to Figure 2. Endoderm Culture Without Lung Scaffold Does Not Promote Differentiation to a Lung Phenotype

(A) Schematic representation of alternate scaffold recellularization. Sorted endodermal cells are seeded on specific matrix proteins, Matrigel or decellularized kidney scaffolds and cultured at air-liquid interface in base supportive media. **(B-C)** H&E staining and transmission EM of seeded endodermal cells reveal the inability of isolated matrix proteins and Matrigel to promote differentiation to lung epithelial cells. H&E scale bar=50µm, EM scale bar=2µm. **(D)** Decellularized kidney scaffolds seeded with definitive endoderm and cultured at air liquid interface cannot support the adherence, proliferation, and differentiation of sorted endodermal cells. Scale bar=50µm

Figure S5, Related to Figure 4. Enzymatic Treatment of Acellular Scaffolds with Heparitinase I Cleaves Heparan Sulfate Proteoglycans.

(A) Natural, acellular and heparitinase I-treated acellular scaffolds were stained for heparan sulfate using biotinylated tomato lectin. Immunostaining reveals the effective cleavage of heparan sulfate proteoglycans following heparitinase I treatment. Scale bar=25µm. **(B)** Cleaved heparan sulfate from scaffolds is detected in the remaining supernatant following heparitinase I treatment using UV spectral analysis for optical density at 232nm. This confirms the efficacy of the enzymatic treatment and removal of heparan sulfate proteoglycans from scaffolds. N=3 experiments; mean ± SEM, *$p<0.01$. **(C-D)** Immunostaining for laminin and collagen IV reveals that the basement membrane remains intact following enzymatic treatment with heparitinase I and chondroitinase ABC. Scale bar=50µm.

Movie S1 – Beating Ciliated Cells in Mature Cultures, Related to Figure 3.

Antibody Information

Target	Host, Conjugation	Company	Catalogue Number	Application, Dilution
Primary Antibodies				
CDH1	Mouse, non-conjugated	BD Biosciences	610181	IF, 1:100
CFTR	Rabbit, non-conjugated	Abcam	Ab181782	IF, 1:200
c-KIT	Rat, PE-Cy7	BD Biosciences	558163	FACS, 1:100
CLDN10	Rabbit, non-conjugated	Santa Cruz	sc-25710	IF, 1:350
Collagen I	Rabbit, non-conjugated	Abcam	ab34710	IF, 1:200
Collagen IV	Rabbit, non-conjugated	Abcam	ab6586	IF, 1:200
CXCR4	Rat, APC	BD Biosciences	558644	FACS, 1:100
Fibronectin	Rabbit, non-conjugated	Abcam	ab23750	IF, 1:200
FOXA2	Mouse, non-conjugated	Abcam	ab60721	1:200
FOXJ1	Goat, non-conjugated	Santa Cruz	sc-54371	IF, 1:200
HSPG	Rat, non-conjugated	Abcam	ab2501	IF, 1:100
Ki67	Rat, non-conjugated	DAKO	M7249	IHC, 1:100
pan-KRT	Rabbit, non-conjugated	DAKO	ZO622	IF, 1:800
KRT5	Rabbit, non-conjugated	Abcam	ab24647	IF, 1:1000
Laminin	Rabbit, non-conjugated	Novus Biologicals	NB300-144	IF, 1:200 WB, 1:1000
NKX2-1	Rabbit, non-conjugated	Abcam	ab76013	1:200
POU5F1	Rabbit, non-conjugated	Cell Signaling	2788-s	1:200
SCGB1A1	Goat, non-conjugated	Santa Cruz	sc-9772	IF, 1:1000 WB, 1:1000
SOX2	Goat, non-conjugated	R&D Systems	AF2018	IF, 1:400
SOX9	Goat, non-conjugated	R&D Systems	AF3075	IF, 1:400
TJN1	Rabbit, non-conjugated	Invitrogen	40-2200	IF, 1:200
TRP63	Mouse, non-conjugated	Santa Cruz	sc-8431	IF, 1:200
TUBB4A	Mouse, non-conjugated	BioGenex	MU178-UC	IF, 1:500
Secondary Antibodies				
Goat IgG	Donkey, Alexa Fluor 647	Invitrogen	A-31573	1:200
Goat IgG	Donkey, Alexa Fluor 488	Invitrogen	A-21202	1:200
Mouse IgG	Donkey, Alexa Fluor 488	Invitrogen	A-11055	1:200
Rabbit IgG	Donkey, Alexa Fluor 546	Invitrogen	A-11056	1:200
Rat IgG	Goat, Alexa Fluor 488	Invitrogen	A-11006	1:200

FACS: Fluorescence-activated cell sorting; IF: Immunofluorescent staining; WB: Western blot

RT-PCR Primers

Gene	Primer Source, Catalogue Number / sequence	
Alb	CCTAGGAAGAGTGGGCACCAAGTGT	AGCAGAGAAGCATGGCCGCCTTTC
Aqp5	TATCCATTGGCTTGTCGGTCAC	TCAGCGAGGAGGGGAAAAGCAAGTA
Cftr	Qiagen, QT00114604	
Foxa2	AAAGTATGCTGGGAGCCGTGAA	CGCGGACATGCTCATGTATGTGTT
Foxa3	Qiagen, QT01657705	
Foxj1	Qiagen, QT00111097	
Muc5ac	Qiagen, QT01196006	
Nkx2-1	TATGCTTCATGGCCCTGAACT	TTTCCTATCTCCAGCGTCTGTCCT
Olig2	AATGCGCGATGCGAAGCTCTTT	AAGCCCACGTTGTAATGCAGGT
Pax8	TCGACTCACAGAGCAGCAGCAGT	AGGTTGCGTCCCAGAGGTGTATT
Pdx1	Qiagen, QT00102235	
Scgb1a1	TCCGCTTCTGCAGAGATCTG	TGAAGAGAGCAACAGCTTTG
Sftpb	Qiagen, QT01537529	
Sftpc	Qiagen, QT00109424	
Sox2	Qiagen, QT01539055	
Sox9	Qiagen, QT00163765	
Tg	Qiagen, QT00116592	
Trp63	Qiagen, QT00197904	

SUPPLEMENTAL EXPERIMENTAL PROCEDURES

ESC Culture and Endoderm Induction

Mouse ESC lines (R1 (*Nkx2-1*^{mCherry})(Bilodeau et al., 2014), G4 (*dsRed-MST*), and129/Ola (*Bry-GFP*/*Foxa2-hCD4*)) and rat ESC line (DAc8) were maintained below passage 40, in the pluripotent state under feeder-free, serum-free culture using 2i conditions as outlined in previously published reports (Ying et al., 2008). The 2i media base consists of DMEM/F12 and Neurobasal Medium (GIBCO) in a 1:1 ratio. This is supplemented with B-27 (with RA) and N-2 supplements (GIBCO), fraction V bovine serum albumin (GIBCO), penicillin/streptomycin (GIBCO), Glutamax (GIBCO), 4μM monothioglycerol (sigma), 1000U/mL LIF (Millipore), 1μM PD0325901 (Stemgent), and 3μM CHIR99021 (Stemgent). Endoderm induction was achieved using a four day embryoid body (EB) culture method with activin A treatment previously outlined in published reports (Gouon-Evans et al., 2006) using serum-free differentiation medium (SFDM). Single cells were seeded at a 20,000 cells/ml density in low adherent plates (Nunc, Roskilde, Denmark) to allow for EB formation for 48 hours. Day 2 EBs were collected and reseeded at 1:2 density in SFDM supplemented with 50ng/ml activin A for an additional 48 hours. Day 4 EBs were harvested and sorted by fluorescence activated cell sorting for cKIT^{+}/CXCR4^{+} cells representing definitive endoderm.

Anterior endoderm was generated for use in RT-PCR as a control. Anteriorization was achieved by seeding sorted definitive endoderm cells as a monolayer on gelatin coated 6-well plates in SFDM supplemented with 10μM SB431542 (Sigma, 431542) and 100ng/ml Noggin (R&D Systems, 1967-NV/CF) for 24hours. Anteriorization was confirmed using RT-PCR analysis showing a reduction in *Foxa3* expression (posterior endoderm).

Decellularization of Lungs

All animal experiments were approved and carried out in accordance with the animal care committee guidelines of the Hospital for Sick Children Research Institute. Decellularization of mouse and rat lung scaffolds was achieved by sequential tracheal lavages and retrograde pulmonary arterial perfusion using a CHAPS-based decellularization solution, without requiring a bioreactor. The heart and lungs were

accessed by a median sternotomy and the trachea was cannulated with a plastic catheter near the thyroid cartilage and secured in place with a suture. Lungs were inflated with phosphate buffered saline (PBS)(no Ca^{2+} and Mg^{2+}) via the tracheal catheter to total lung capacity to assist perfusion (<12 cmH_2O in mice, <20 cmH_2O in rats). A 25-gauge syringe inserted through the right ventricle was used to access the pulmonary artery and allow perfusion with 10U/mL heparinized HBSS- (Sigma, H0777) to remove blood cells. The inferior vena cava was ligated and the left atrium slit to indirectly drain the pulmonary veins. The lungs were decellularized with sequential tracheal lavages (10 lavages) with decellularization solution (8mM CHAPS, 25mM EDTA, 1M NaCl in PBS), followed by extensive rinsing with PBS (10-15 lavages). Lungs were then removed from the animal and exposed to 90U/ml Benzonase endonuclease (Novagen, 70664-3) for 12 hours while on a rotator at room temperature to remove cellular components. Scaffolds were then treated with antimicrobial agents, 200U/mL pen/strep (Gibco, 15140) and 25µg/mL amphotericin B (Gibco, 15290) for 6 hours at room temperature to prepare for recellularization. Thick vibratome sections (Leica) of acellular lung were generated at approximately 350µm and conditioned with SFDM media prior to recellularization.

Recellularization of Thick Scaffold Sections

Thick sections of decellularized lung were transferred to Nucleopore hydrophobic floating membranes (8µm pore size, Whatman, 110614) and seeded with 100,000cells/section using sorted $cKIT^+/CXCR4^+$ endodermal cells. Cultures were maintained in 6-well plates in SFDM, without any additional inductive factors. Media was changed every 48 hours for up to 21 days.

DNA Assay

For DNA assay, DNA was extracted from decellularized lung scaffolds using a chloroform/phenol extraction method. DNA was measured by UV absorbance in microplates using a SpectraMax Absorbance Microplate Reader equipped with SoftMax Pro Data Acquisition & Analysis software.

Tensile Testing

Natural and decellularized sections of lung underwent tensile testing using Mach-1 Motion setup and software (Biosyntech). Sample sections (1-2cm^2 cross-sectional area and 500µm thick) were stretched until break point to assess the ultimate tensile strength, represented by stress-strain curves.

Immunostaining

Cell-scaffold cultures were fixed in 4% paraformaldehyde (PFA) at 4°C for 8 hours. Samples were paraffin embedded and sectioned at 5µm. Sample sections were rehydrated and heat-induced epitope retrieval with citrate buffer was performed. Slides were then blocked for one hour with 5% normal donkey serum and 1% BSA in PBS for 1 hour at room temperature. Samples were then incubated with primary antibodies at 4°C overnight in humidified chamber, and detected using Alexa Fluor conjugated secondary antibodies (Invitrogen) for one hour at room temperature. Nuclei were counterstained using DAPI (Invitrogen). Details of antibodies are provided in the Antibody Table. Images were captured with Leica CTRMIC 6000 confocal microscope and Hamamatsu C910013 spinning disc camera (Leica Microsystems Inc.), and analyzed with Volocity software (PerkinElmer).

For immunohistochemical stain of Ki67, sections were rehydrated and heat-induced epitope retrieval with citrate buffer was performed. Sections were immunostained for Ki67 expression using a standard procedures with a Ki-67 primary antibody diluted in blocking buffer and incubated overnight at 4°C in humidified chamber. Slides were washed thoroughly with PBS and primary antibody was detected by using biotinylated rabbit anti-rat secondary antibody (Jackson ImmunoResearch) diluted 1:200, followed by ABC kit (from Vector). The color was developed by addition of diaminobenzidine (DAB) (Sigma) and counterstained with Mayer's hematoxylin (Sigma, H9627).

For transferase (TdT)-mediated dUTP nick end labeling (TUNEL) of apoptotic cells, tissue slides were rehydrated and antigen retrieval was completed as stated above. Assay was completed as per manufacturer's protocol using TUNEL enzyme (Roche, 11767305001) and TUNEL Label Mix (Roche, 11767291910).

Flow cytometry and cell sorting

For definitive endoderm, day 4 EBs were dissociated using TrypLE express (Gibco), for 3 minutes at 37°C. Single cell suspensions were labeled with cKIT and CXCR4 antibodies in Sort Buffer (Hank's balanced salt solution (HBSS-) supplemented with 2% (v/v) fetal bovine serum and 10mM HEPES buffer) for 20 minutes on ice. Cells were sorted using AriaII-GC (BD Biosciences) and data analysis was carried out using Diva (BD Biosciences) and FlowJo (TreeStar) software.

For identification of mcherry positive cells differentiated on scaffolds, day 7, 14, and 21 cultures were dissociated to isolate seeded cells for flow cytometric quantification. Cell-scaffold tissue cultures were incubated in an elastase solution (1mg/mL elastase in SFDM with 2% fetal bovine serum (FBS)), at 37°C for 30 minutes. Tissue was spun to remove elastase, and placed in FBS with 2.5% DNAse and minced for one minute at 4°C, followed by vigorous shaking for 2 minutes to aid in releasing of cells. SFDM was added to mixture, and minced tissue was filtered using a pre-wetted 20µm nylon mesh filter. Cellular recovery using this method were as follows, day 7 cultures: $3.63x10^5 \pm 1.1x10^4$ (n=3), day 14 cultures: $4.55x10^5 \pm 5.3x10^4$ (n=3), day 21 cultures: $9.43x10^5 \pm 1.9x10^4$ (n=3). Cells were collected into Sort Buffer and analyzed for mcherry expression using a MoFlo (Beckman Coulter) apparatus and Diva (BD Biosciences) software.

Real Time Quantitative PCR

RNA was extracted from cell-scaffold cultures using PicoPure RNA Isolation Kit (Life Technologies), and cDNA synthesis was carried out with 1ng of RNA using SuperScript III Reverse Transcriptase (Invitrogen), according to the manufacturer's protocol. Ten micrograms of template cDNA was used for real-time PCR (40 cycles of amplification) using SYBR GreenER qPCR SuperMix with murine specific primer sets, listed in RT-PCR Primer Table. Analysis was performed using StepOnePlus qPCR (Applied Biosystems). Gene expression was normalized to RNA Polymerase II and expressed relative to selected positive (adult tissue, E13 lung) or negative controls (definitive endoderm).

Immunoblot Analysis

For laminin detection, 50µg of solubilized extracellular matrix supernatant (in RIPA buffer), and 1µg of purified laminin protein as positive control, were separated on a 5% SDS-PAGE gel. For SCGB1A1 detection, 50µg of day 21 cell-scaffold culture media, and rat lung lysate as positive control, were separated on a 3%–12% gradient SDS-PAGE gel (Invitrogen). Proteins were transferred to nitrocellulose paper (Millipore) and blocked with 3% milk in PBS plus 0.1% Tween-20. The membranes were then incubated overnight at 4°C with anti-laminin or anti-SCGB1A1 antibodies at 1:1000 dilution in PBS-milk 1% containing 0.2% Tween-20. Blots were then incubated for 1 hour with respective secondary antibodies conjugated with peroxidase, and were developed using chemiluminescent substrates (PerkinElmer) according to the manufacturer's instructions and imaged on X-ray film.

Histological Analysis

Cell-scaffold cultures were fixed in 4% paraformaldehyde (PFA) at 4°C for 8 hours. Samples were paraffin embedded and sectioned at 5µm. Slides were rehydrated and standard hematoxylin and eosin staining, Hart's elastin stain, and periodic acid-Schiff (PAS) stain was performed.

Electron Microscope Analysis

Samples were fixed in 2.5% glutaraldehyde in 0.1M phosphate buffer pH7.4. Transmission EM specimens were post-fixed in osmium tetroxide, dehydrated in an ascending series of acetone, infiltrated and embedded in Epon Araldite prior to polymerization at 60° C overnight. Ultrathin sections were then cut and mounted on grids, and stained with uranyl acetate and lead citrate prior to microscopy (JEOL, JEM1011) and image acquisition was completed using a CCD camera (AMT corp.). Scanning EM samples were post-fixed in osmium tetroxide, dehydrated in an ascending series of ethanols and critical point dried. Samples were then mounted on aluminum stubs using double-sided carbon tape. Samples were rendered conductive with a thin coat of gold palladium using a sputter coater and examined and photographed in a field emission scanning EM (JEOL, JSM 6700F).

Efflux Assay

Iodide efflux from differentiated cultures following cAMP agonist stimulation was measured periodically to assess CFTR channel activity, as CFTR is permeable to iodide. Day 21 scaffold cultures were loaded with sodium iodide solution (3.0mM KNO_3, 2.0mM $Ca(NO_3)_2$, 11mM glucose, 20mM HEPES, 136mM NaI) in a 6-well plate for 1h at 37°C, for iodide uptake (three cell-scaffold cultures were pooled for each assay) measurements. Samples were then washed 10 times with wash solution (3.0mM KNO_3, 2.0mM $Ca(NO_3)_2$, 11mM glucose, 20mM HEPES, 136mM $NaNO_3$) and epithelium sodium channel (ENaC)-specific inhibitor amiloride (100µM). The last wash was collected as a blank reading, followed by eight sequential readings of cAMP-stimulated halide flux using 300µl of wash solution containing FIG (10µM forskolin, 100µM 3-isobutyl-1-methylxanthine, and 50µM genistein). Each reading represented 1 minute of exposure to FIG wash solution. Vehicle dimethyl sulfoxide (DMSO) was used as a negative control reading. Solutions from each one-minute time point were collected into a 96 well plate and absolute iodide electrode potential value (mV) was measured using a halide-selective microelectrode (Lazar Research Laboratories). Readings were recorded using Digidata 1320A Data Acquisition System and Clampex 8.1 software. Using a calibration curve, recorded mV values were converted to iodide concentration in µM.

Enzymatic Treatment of Scaffolds

Decellularized scaffolds were treated with Heparitinase I solution (0.1M sodium acetate, 10mM calcium acetate, 10mU heparitinase I (Amsbio, 100704)) for 4 hours at 37°C. Enzymatic activity was confirmed by UV spectral analysis of treated scaffolds at 232nm for HS disaccharides in the wash supernatant, as well as Tomato-lectin staining (Vector Laboratories, B-1175 1:500 dilution; detection with PE-conjugated Streptavidin, Biolegend, 405203 1:200 dilution) of the untreated and treated scaffolds. Alternatively, scaffolds were treated with chondroitinase ABC solution (0.4M Tris-HCl buffer pH8.0, 0.4M sodium acetate, 0.1% BSA, 5mU chondroitinase ABC (Amsbio, 100330-1A) for 1 hour at 37°C. Enzymatic activity was confirmed by immunoblot analysis for removal of CS proteoglycans from treated scaffolds. Following enzymatic treatment, scaffolds were

rinsed first with PBS (containing penicillin-streptomycin and amphotericin B) for one hour, followed by SFDM media. Sorted endodermal cells were seeded on scaffolds and cultured at air liquid interface as previously described.

Protein Profiler Array

A protein antibody array (R&D Systems, ARY015) was used to identify candidate analytes remaining on decellularized scaffolds, as per manufacturer's instructions. Briefly, following decellularization, scaffolds treated with or without heparitinase I were homogenized in PBS with protease inhibitors. After homogenization, 1% triton X-100 was added to samples. Samples underwent one freeze-thaw cycle and were then centrifuged at 10,000 x g for 5 minutes to remove cellular debris. Protein concentration was determined using Bradford protein assay (Bio-rad). Sample lysates were diluted (300µg of protein per sample), mixed with a cocktail of biotinylated detection antibodies, and incubated overnight with the protein array membrane. Streptavidin-HRP and chemiluminescent detection reagents were used for detection. A signal was generated at each capture spot on membrane, corresponding to the amount of protein bound. Pixel density for each spot was detected and quantified using ImageJ open access software.

Kidney Scaffold Decellularization

Adult mouse kidneys were sectioned to 1000µm using a vibratome (Leica). Sections were soaked in 0.1% SDS using a peristaltic pump supplying fresh SDS at a flow rate range of 0.4-0.8 rpm for 72 hours. Decellularized kidney scaffolds were soaked in 100x Pen/Strep for 1 hour to remove any contaminates. Scaffolds were then washed with PBS and SFDM prior to seeding with sorted $cKIT^{+}/CXCR4^{+}$ endodermal cells.

Endoderm Culture on Isolated Matrix Proteins

Sorted endodermal cells were seeded onto isolate matrix proteins and cultured under the same conditions as with seeded lung scaffolds in SFDM, at air liquid interface using the hydrophobic floating membranes (Whatman, 110614). Matrix proteins used include mouse laminin (BD, 354232), human fibronectin (BD, 356008), rat-tail collagen I (BD, 356236), and mouse collagen IV (BD, 354233). Matrix proteins were diluted to 10µg/mL

and applied to the floating membranes prior to seeding with endoderm. For Matrigel (BD, 356230), a thick coat (200µl) was placed on floating membranes and allowed to gel prior to seeding with endoderm.

Statistical Analysis

Statistical comparisons were performed using unpaired t-tests, unless specified otherwise. For multiple comparisons of more than two groups, one-way ANOVA was used with Dunnett's test for significance.

Supplemental References

Bilodeau, M., Shojaie, S., Ackerley, C., Post, M., Rossant, J., 2014. Identification of a Proximal Progenitor Population from Murine Fetal Lungs with Clonogenic and Multilineage Differentiation Potential. Stem Cell Reports 3, 1–16.

Gouon-Evans, V., Boussemart, L., Gadue, P., Nierhoff, D., Koehler, C.I., Kubo, A., Shafritz, D.A., Keller, G., 2006. BMP-4 is required for hepatic specification of mouse embryonic stem cell–derived definitive endoderm. Nature Biotechnology 24, 1402–1411.

Ying, Q.-L., Wray, J., Nichols, J., Batlle-Morera, L., Doble, B., Woodgett, J., Cohen, P., Smith, A., 2008. The ground state of embryonic stem cell self-renewal. Nature 453, 519–523.